

NAVAL POSTGRADUATE SCHOOL  
Monterey, California

AD-A243 408



DTIC  
SELECTE  
DEC 17 1991  
S D D



THESIS

THE EFFECT OF TITANIUM INCLUSIONS  
ON HY-80 GMA WELD DEPOSITS

by

David J. Ellis

December, 1990

Thesis Advisor:

Alan G. Fox

Approved for public release; distribution is unlimited.

91-18083



20000 901010

91 1216 037

Unclassified

security classification of this page

REPORT DOCUMENTATION PAGE				
1a Report Security Classification <b>Unclassified</b>		1b Restrictive Markings		
2a Security Classification Authority		3 Distribution Availability of Report Approved for public release; distribution is unlimited.		
2b Declassification Downgrading Schedule				
4 Performing Organization Report Number(s)		5 Monitoring Organization Report Number(s)		
6a Name of Performing Organization Naval Postgraduate School	6b Office Symbol (if applicable) 34	7a Name of Monitoring Organization Naval Postgraduate School		
6c Address (city, state, and ZIP code) Monterey, CA 93943-5000		7b Address (city, state, and ZIP code) Monterey, CA 93943-5000		
8a Name of Funding Sponsoring Organization	8b Office Symbol (if applicable)	9 Procurement Instrument Identification Number		
8c Address (city, state, and ZIP code)		10 Source of Funding Numbers		
		Program Element No	Project No	Task No
		Work Unit Accession No		
11 Title (include security classification) <b>THE EFFECT OF TITANIUM INCLUSIONS ON HY-80 GMA WELD DEPOSITS</b>				
12 Personal Author(s) <b>Dana J. Ellis</b>				
13a Type of Report Master's Thesis	3b Time Covered From: To	14 Date of Report (year, month, day) December 1990	15 Page Count 79	
16 Supplementary Notation The views expressed in this thesis are those of the author and do not reflect the official policy or position of the Department of Defense or the U.S. Government.				
17 Cosau Codes		18 Subject Terms (continue on reverse if necessary and identify by block number)		
Field	Group	Subgroup	Titanium Inclusions, HY-80 GMA Weld Deposits.	
19 Abstract (continue on reverse if necessary and identify by block number)				
<p>HY-80 steels are used in submarine and ship construction and it has been found that small additions of titanium to this steel during manufacture markedly improve the fracture toughness of the heat affected zone (HAZ) of Gas-Metal-Arc-Welding (GMAW) deposits made from this steel. This has been ascribed to prior austenite grain boundary pinning by titanium nitride inclusions.</p> <p>In the present work the weld metals, HAZ and parent metals of GMAW welds made on HY-80 steel have been studied by optical, scanning electron and transmission electron microscopy. These studies have shown that the Ti treated HY-80 has overall a lower level on non-metallic inclusions than untreated HY80 which could certainly be responsible for improved toughness. Unfortunately it proved difficult to correlate titanium nitride inclusions with prior-austenite-grain-boundary pinning.</p>				
20 Distribution Availability of Abstract		21 Abstract Security Classification		
<input checked="" type="checkbox"/> unclassified unlimited <input type="checkbox"/> same as report <input type="checkbox"/> DTIC users		Unclassified		
22a Name of Responsible Individual Alan G. Fox		22b Telephone (include area code) (408) 646-2142	22c Office Symbol ME/Fo	

DD FORM 1473,84 MAR

83 APR edition may be used until exhausted  
All other editions are obsolete

security classification of this page

Unclassified

Approved for public release; distribution is unlimited.

The Effect Of Titanium Inclusions On HY-80  
GMA Weld Deposits

by

Dana J. Ellis  
Lieutenant, United States Navy  
B.S.M.E., Ohio State University, 1981

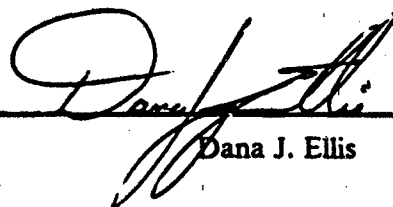
Submitted in partial fulfillment of the  
requirements for the degree of

MASTER OF SCIENCE IN MECHANICAL ENGINEERING

from the

NAVAL POSTGRADUATE SCHOOL  
December 1990

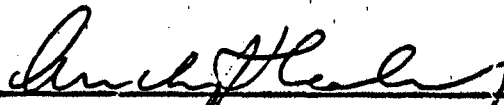
Author:

  
Dana J. Ellis

Approved by:

  
A. G. Fox

Alan G. Fox, Thesis Advisor



Anthony J. Healey, Chairman,  
Department of Mechanical Engineering

## ABSTRACT

HY-80 steels are used in submarine and ship construction and it has been found that small additions of titanium to this steel during manufacture markedly improve the fracture toughness of the heat affected zone (HAZ) of Gas-Metal-Arc-Welding (GMAW) deposits made from this steel. This has been ascribed to prior austenite grain boundary pinning by titanium nitride inclusions.

In the present work the weld metals, HAZ and parent metals of GMAW welds made on HY-80 steels have been studied by optical, scanning electron and transmission electron microscopy. These studies have shown that the Ti treated HY-80 has overall a lower level on non-metallic inclusions than untreated HY80 which could certainly be responsible for improved toughness. Unfortunately it proved difficult to correlate titanium nitride inclusions with prior-austenite-grain-boundary pinning.

Accession For	
NTIS CRA&I	<input checked="checked" type="checkbox"/>
DTIC TAB	<input type="checkbox"/>
Unannounced	<input type="checkbox"/>
Justification	
By	
Distribution /	
Availability Codes	
Dist	Avail and/or Special
A-1	



## TABLE OF CONTENTS

I. INTRODUCTION .....	1
II. BACKGROUND .....	3
A. CHARACTERISTICS OF HY-80 STEEL .....	3
1. Effect of Alloying Elements .....	5
2. Structure-Property Relationships in Bainitic Steels .....	9
3. Inclusions in Steel .....	11
a. Composition of Inclusions in Steel .....	12
b. Relationship between Inclusions and Microstructure .....	13
B. HY-80 WELD METAL .....	13
1. The Microstructure of HY-80 Steel Welds .....	13
2. Cooling Rate and Microstructure .....	14
3. Influence of Titanium on Weld Metal Microstructure and Properties ..	16
4. Inclusions in Weld Metal .....	19
a. Composition of Inclusions in Weld Metal .....	21
b. Relationship between Inclusions and Microstructure .....	21
C. WELDING PROCESS .....	23
1. The GMAW Process .....	23
D. HY-80 HAZ MICROSTRUCTURE .....	26
1. Influence of Titanium on HAZ Microstructure .....	26
E. SCOPE OF PRESENT WORK .....	26
III. EXPERIMENTAL PROCEDURE .....	28
A. MATERIAL .....	28
B. MECHANICAL PROPERTIES .....	28
C. MICROSCOPY .....	28
1. Optical Microscopy .....	28
D. SCANNING ELECTRON MICROSCOPY .....	29
E. TRANSMISSION ELECTRON MICROSCOPY .....	29
IV. RESULTS AND DISCUSSION .....	30

A. MICROSTRUCTURAL OBSERVATION IN HAZ AND PARENT METAL .....	30
B. OPTICAL MICROSCOPY .....	30
C. SCANNING ELECTRON MICROCOPY .....	30
1. SEM Microscopy .....	30
a. Ti Treated HAZ Microstructure .....	30
b. Ti Treated Parent Metal Microstructure .....	32
c. Non-Ti Treated HAZ Microstructure .....	33
d. Non-Ti Treated Parent Metal Microstructure .....	34
e. Ti Treated HAZ Inclusion Micrographs .....	35
f. Ti Treated Parent Metal Inclusion Micrographs .....	41
2. EDX Analysis .....	44
D. TRANSMISSION ELECTRON MICROSCOPY .....	56
1. TEM Microscopy .....	56
a. Ti Treated Parent Metal .....	56
b. Ti Treated HAZ .....	57
E. MECHANICAL PROPERTIES .....	61
V. SUMMARY .....	64
A. CONCLUSIONS .....	64
B. RECOMMENDATIONS .....	64
LIST OF REFERENCES .....	65
INITIAL DISTRIBUTION LIST .....	68

## LIST OF TABLES

Table 1. CHEMICAL COMPOSITION SPECIFICATION LIMITS OF HY-80 STEEL PLATE .....	5
Table 2. CHEMICAL COMPOSITION OF FILLER MATERIAL MIL-100S, . 25	25
Table 3. SUMMARY OF RESULTS .....	60

## LIST OF FIGURES

Figure 1.	TTT Curves for HY-80 .....	4
Figure 2.	Maximum hardness vs. carbon content .....	6
Figure 3.	Effect of oxygen on the notch toughness .....	8
Figure 4.	Effect of oxygen on the Charpy V notch shelf energy .....	9
Figure 5.	The effect of cooling rate on yield strength for GMAW and SMAW ..	15
Figure 6.	Role of Ti formation of acicular ferrite .....	17
Figure 7.	Effects of Ti on weld metal transformation .....	18
Figure 8.	Size distribution of Non-metallic inclusions .....	20
Figure 9.	Ternary phase diagram .....	22
Figure 10.	GMAW Process .....	24
Figure 11.	Montage of Microstructure .....	31
Figure 12.	SEM Micrograph Ti Treated HAZ .....	32
Figure 13.	SEM Micrograph Ti Treated Parent Metal .....	33
Figure 14.	SEM Micrograph Non Ti Treated HAZ Grain Boundaries .....	34
Figure 15.	SEM Micrograph Non Ti Treated Parent Metal Grain Boundaries ...	35
Figure 16.	SEM Micrograph Ti Treated HAZ .....	36
Figure 17.	SEM Micrograph Ti Treated HAZ .....	37
Figure 18.	EDX Analysis multiphase TiZrN inclusion .....	38
Figure 19.	SEM Micrograph Ti Treated HAZ .....	39
Figure 20.	EDX Analysis multiphase CaAlTiMgO inclusion .....	40
Figure 21.	SEM Micrograph Ti Treated Parent Metal .....	41
Figure 22.	SEM Micrograph Non Ti Treated Parent Metal .....	42
Figure 23.	SEM Micrograph Ti Treated Parent Metal .....	43
Figure 24.	SEM Micrograph Ti Treated Parent Metal TiN inclusion .....	44
Figure 25.	Oxide Inclusion distribution Non Ti Treated Parent Metal .....	46
Figure 26.	Sulfide Inclusion distribution Non Ti Treated Parent Metal .....	47
Figure 27.	Oxide Inclusion distribution Non Ti Treated Parent, HAZ, Weld ....	48
Figure 28.	Sulfide Inclusion distribution Non Ti Treated Parent, HAZ, Weld ....	49
Figure 29.	Oxide Inclusion distribution Ti Treated Parent Metal .....	50
Figure 30.	Sulfide Inclusion distribution Ti Treated Parent Metal .....	51
Figure 31.	Nitride Inclusion distribution Ti Treated Parent Metal .....	52



Figure 32.	Oxide inclusion distribution Ti Treated HAZ, Weld, Parent .....	53
Figure 33.	Sulfide inclusion distribution Ti Treated HAZ, Weld, Parent .....	54
Figure 34.	Nitride inclusion distribution Ti Treated HAZ, Weld, Parent .....	55
Figure 35.	TEM Micrograph Ti Treated Parent Metal .....	56
Figure 36.	TEM Micrograph Ti Treated Parent Metal .....	57
Figure 37.	TEM Micrograph Ti Treated Parent Metal .....	57
Figure 38.	TEM Micrograph Ti Treated HAZ .....	58
Figure 39.	TEM Micrograph Ti Treated HAZ .....	58
Figure 40.	TEM Micrograph Ti Treated HAZ .....	59
Figure 41.	Charpy V-notch impact energy Ti-treated .....	62
Figure 42.	Charpy V-notch impact energy non Ti-treated .....	63

## ACKNOWLEDGMENT

I would like to thank Professor Alan G. Fox for his technical guidance and assistance of this thesis. I would also like to thank Elisabeth Grayson for her technical support.

## I. INTRODUCTION

In the mid 1950's design requirements were for a steel of 540 MPa yield strength for plating and framing in pressure hull structures of new submarines. This required that the steel have adequate strength, ductility and notch toughness. Also, the steel needed to possess good weldability and the weld deposit would be of adequate strength and notch toughness. The initial research and development work to formulate a steel with the required mechanical properties and welding behavior resulted in the development of the quenched and tempered (QT) low alloy steel QT35 which, until 1966 was used for submarine construction in the UK. In the United States a similar design led to the introduction to HY-80 (High Yield). Changes in the specification since the first design have lowered the maximum allowable carbon content and also introduced minimum values of manganese, silicon, nickel, molybdenum, sulphur, and phosphorus.

The effects of a small amount of Titanium to control grain size on increasing the toughness of HY-80 and High Strength Low Alloy (HSLA) steel has become of particular interest to the U.S. Navy in recent years. A major factor is cost savings through use of these steels for Naval Construction due to these higher strength steels to notch toughness and reduction or elimination of preheat for welding.

HY-80 steel is a quenched and tempered, low carbon, nickel, chromium-molybdenum steel. Manganese, silicon, aluminum, and calcium are added during the steel making process in order to counteract the deleterious effects of sulphur and oxygen by combining with them to form compounds which float out of large inclusions. Those remaining are small, hard and remain in the steel as non-metallic inclusions. The addition of titanium to high strength steel weld metal improves its toughness and that the improvements are due to a refinement in microstructure [Ref. 1]. Titanium most often

combines with nitrogen or oxygen which promotes intergranular nucleation of acicular ferrite. Also, it is the inclusion size and distribution which is the basis for the nucleation of ferrite, and is fundamental to the microstructural properties. As a result, the control of microstructure with a maximum resistance to cleavage is an important factor as the strength of Naval construction steels increase.

Attempts to control the weld metal acicular ferrite content has led to welding consumables containing deoxidizers (Ti, Al, Si, Mn) and a balance of alloying elements such as (V, Cu, Nb, Cr, Mo, B). Additions of other hardenability elements may be used to ensure the desired strength level by solid solution or precipitation strengthening, and to control the microstructure through nucleation and growth in order to optimize the weld metals strength.

In Gas Metal Arc deposits the toughness of the low C-alloy steel is effected by its microstructure, produced through the transformation in cooling process. The Heat Affected Zone (HAZ) undergoes microstructural transformations due to thermal cycling that occurs in the welding process. For this reason the development of the understanding the role of inclusions in the weld metal phase transformation with mechanical properties of Titanium treated and untreated HY-80 Ship Building Steels are critical in the certification of High Strength Low Alloy Steels for Naval ship construction.

In the present work the weld metals, HAZ and parent metals of GMAW welds made on HY-80 steels have been studied by optical, scanning electron and transmission electron microscopy. With a view to understanding the improvements in HAZ toughness which is apparent in multirun GMAW steels when small amounts of Ti are present.

## II. BACKGROUND

### A. CHARACTERISTICS OF HY-80 STEEL

HY-80 steel is a low carbon alloy steel quenched and tempered to achieve a yield strength of 552 MPa. This low carbon, nickel-chromium-molybdenum steel, developed by the U.S. Steel Corporation in cooperation with the U.S. Navy for ship construction. The principal advantage of the high yield steels are their high strength and toughness over a wide temperature and their good weldability. HY steels develop their high strength from quench and temper heat treatment which leads to a tempered bainite-martensite microstructure.

The Time-Temperature-Transformation diagram shown in Figure 1 on page 4 illustrates, these transformations as a function of austenitizing temperature. Heat treatments for HY-80 generally consist of austenitization at approximately 890 C followed by a water quench and tempering in the range of 621 C to 678 C followed by water quench [Ref. 2].

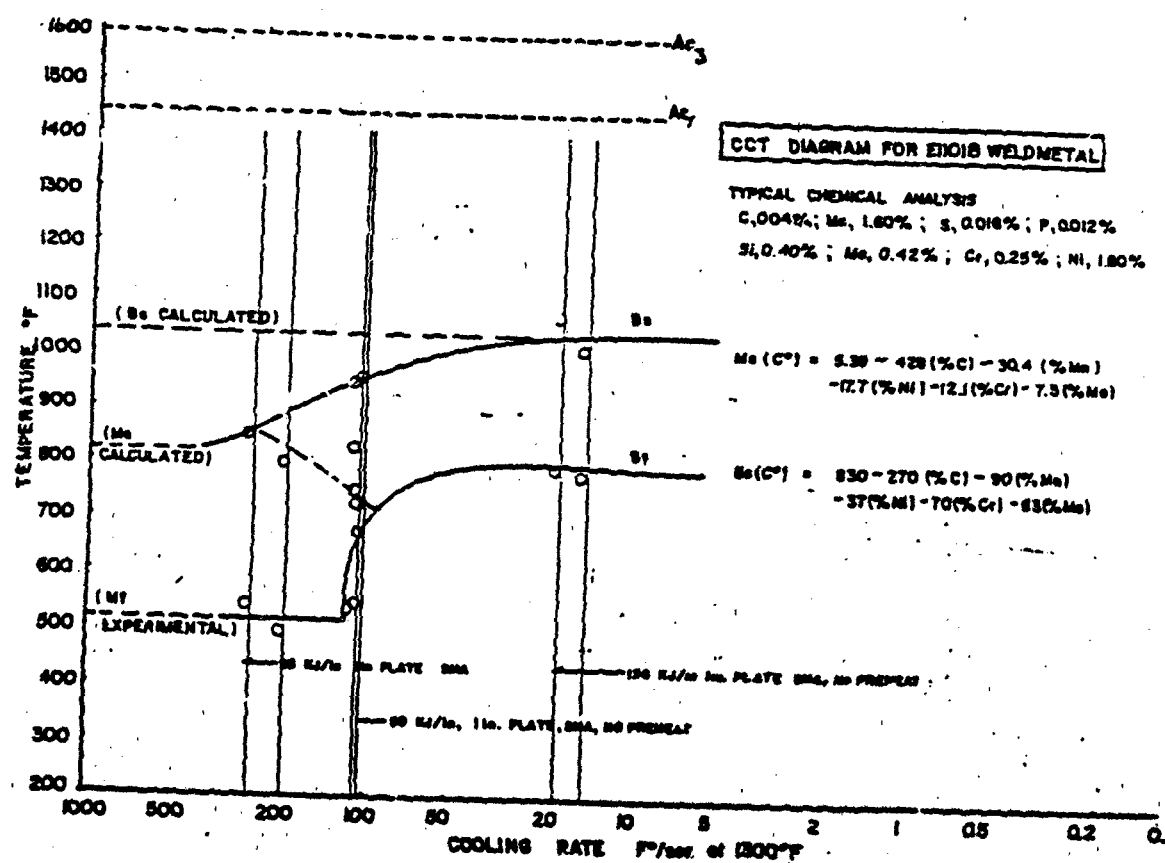


Figure 1. TTT Curves for HY-80 (provided by David Taylor Naval Research and Development Center)

HY-80 is in a general class of high strength steels called low-carbon martensite, which contain less than 0.18 percent carbon to ensure good weldability. Also, alloying elements such as silicon, nickel, chromium, molybdenum, vanadium, titanium, and copper which serve an important role in establishing the mechanical properties of HY-80. The chemical composition specifications of the HY-80 steel plate used in this investigation are shown in Table 1.

**Table 1. CHEMICAL COMPOSITION SPECIFICATION LIMITS OF HY-80 STEEL PLATE (weight percent). Major elements for heavy gage plate, greater than one inch.**

ELEMENT	HY-80 MIL-S-162-16J
C	0.13-0.18
Mn	0.10-0.40
P	0.015
S	0.008
Si	0.015-0.38
Ni	2.50-3.50
Cr	1.40-1.80
Mo	0.35-0.60
Cu	0.25

Close control of deleterious elements such as sulfur and phosphorus is important.

#### 1. Effect of Alloying Elements

The type and amounts of alloying elements present in a steel determine the properties of the finished product. The effect of common alloying elements in low alloy steels will be discussed below, with emphasis on their role in HY steel.: (Ref. 3)

- Carbon

Carbon is generally the most important alloying element in steels. The addition of carbon is an inexpensive and efficient method of increasing the strength of steels and this is accomplished via two methods. First, increases in the carbon content will increase the hardenability, or the ease of formation of martensite, of a particular steel. The formation of products such as bainite or martensite greatly increases the strength level of the steel. In addition to increased hardenability, increasing carbon content increases strength by forming a greater percentage of

pearlite, or by increasing the strength of any martensite or bainite formed. Unfortunately, this increased strength is accompanied by decreases in both ductility and toughness.

In alloy steels the effect of carbon on hardenability is minor when compared to the effect of other elements. Once lower temperature transformation products are formed, however, carbon plays an important role in determination of the final properties. Figure 2 illustrates, the hardness of martensite (After Burns, et al; [Ref. 4]) formed, is directly related to the carbon content and this holds true for both plain carbon and alloy steels. To optimize the balance between strength and toughness, the carbon content should be kept at the lowest level necessary to obtain the desired strength [Ref. 5].

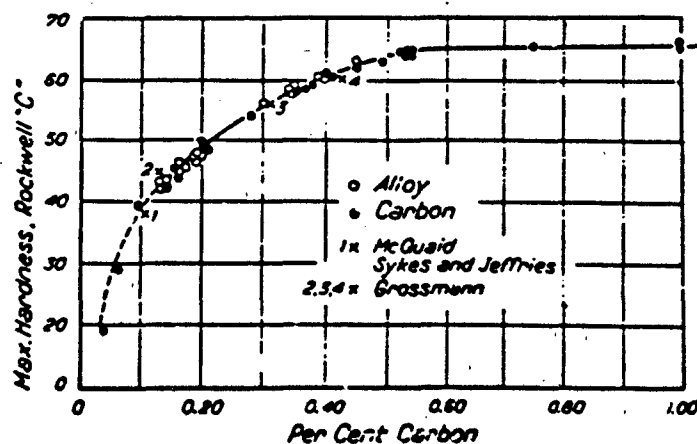


Figure 2. Maximum hardness vs. carbon content

From a welding point of view it is desirable to keep the carbon content to a minimum to reduce the tendency for cracking. This is often caused when the carbon content is greater than 0.01 percent which causes sulphur to be rejected at the grain boundaries of primary austenite grains, promoting intergranular weakness and solidification cracking. [Ref. 3]

- **Manganese**

The major role of manganese in steels is to tie up an sulfur present as impurities. The amount of manganese necessary for this purpose is generally about 30 times the percentage of sulfur present. Manganese also contributes to increased



hardenability and may have either a beneficial or detrimental effects on toughness, depending on the steel and its heat treatment [Ref. 6]. In high strength weld metal a higher manganese content is found to be necessary, and Dorsch and Lesnwich recommended a level of 1.9% to 2.2% when a preheat of 93 C is used [Ref. 7]. Higher levels were found to promote cracking and embrittlement, particularly when the carbon content was high. In addition manganese prevents the formation of harmful FeS at grain boundaries by reacting with dissolved sulfur to form MnS. These MnS inclusions are deformed during the rolling process associated with structural steels. Rare earth additions or Ca can be used to control the shape and strength of these inclusions. [Ref. 3]

- **Nickel**

Nickel has a moderate effect in increasing both yield and ultimate strength. The disadvantages of adding nickel are increased cost and a slight increase in hot cracking susceptibility [Ref. 7].

The actual level where cracking occurs is affected by other elements, with higher sulfur and phosphorus contents resulting in a lower tolerance for Ni [Ref. 6]. The latter is the reason for the much lower nickel contents in fillers developed for HY Steels. The additions of Ni increase the strength and toughness by solid solution strengthening and decrease the ductile to brittle transition temperature (DBTT). [Ref. 3]

- **Chromium**

In the concentrations present in low alloy steels chromium is effective in increasing hardenability and promoting the formation of lower bainite [Ref. 7]. It has a moderate effect in increasing yield and ultimate strength, although the tensile ductility and notch toughness may be reduced [Ref. 6]. Chromium is also reported to have an adverse on toughness when used as a substitute for molybdenum or nickel in the amounts necessary to maintain a given strength level [Ref. 6]. It is a moderate carbide former and can increase the susceptibility of HY steel to temper embrittlement when present in amounts greater than 1% [Ref. 5]. [Ref. 3]

- **Molybdenum**

In many ways the effects of molybdenum are similar to those of chromium, although it is slightly more effective in increasing hardenability [Ref. 7]. At higher levels molybdenum was found to promote embrittlement, with the actual level dependent on the manganese and chromium levels [Ref. 7]. In filler metal development a level of 0.4% was required to provide a "bainitic shelf", while levels above 0.6% were detrimental to weld properties [Ref. 7]. [Ref. 3]

- **Silicon**

The main role of silicon is prevention of porosity by deoxidation during steelmaking or welding. The effect on hardenability is controversial, although it is generally accepted that silicon increases the fluidity of the weld pool. While the actual value varies, it is the consensus of the literature that excessive silicon reduces the toughness of low alloy steels [Ref. 6]. [Ref. 3]

- **Vanadium**

Vanadium is a very strong carbide former and is sometimes added for secondary hardening. It was found to be necessary to add a small amount of vanadium to HY steel to retard the loss of strength on tempering. Vanadium in concentrations greater than 0.010% can promote temper embrittlement and alloys in this category are not recommended where stress relief is required. [Ref. 3]

- Sulfur and Phosphorus

Sulfur and phosphorus are generally regarded as impurities in steels. As the strength level of a steel increased, the tolerance for these elements decreases dramatically, and this shows up as a decrease in toughness. These elements can also contribute to hot cracking. [Ref. 3]

- Oxygen and Nitrogen

High strength steels are also very sensitive to contamination from oxygen and nitrogen. Because there are many potential sources of contamination, these are of great concern in welding. Figure 3 illustrates, and Figure 4 on page 9 and increase in the oxygen content degraded the toughness by both lowering the lower shelf energy absorption and increasing the 50 ft-lb transition temperature.

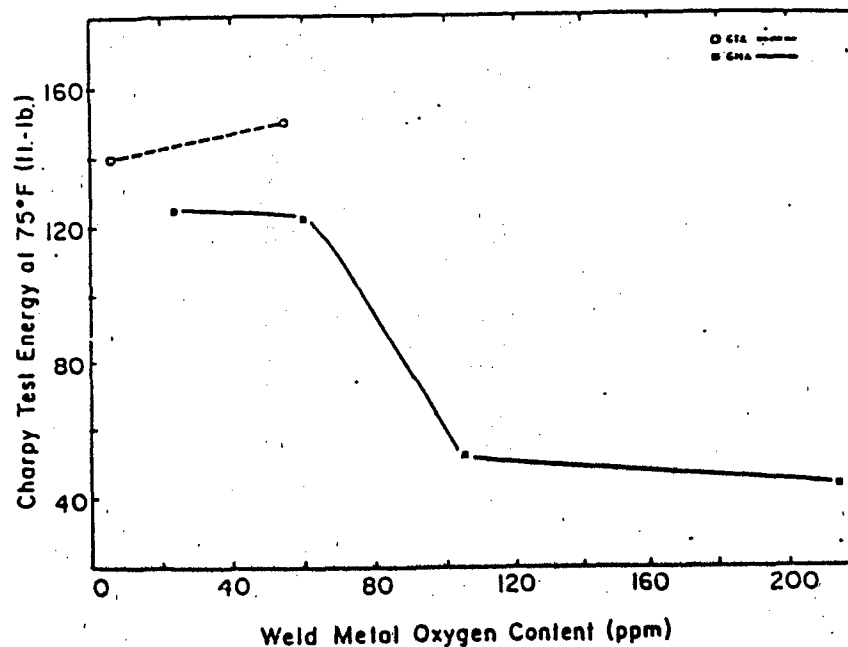


Figure 3. Effect of oxygen on the notch toughness transition temperature in a 3% nickel weld metal. (after Stout, et al; [Ref. 8])

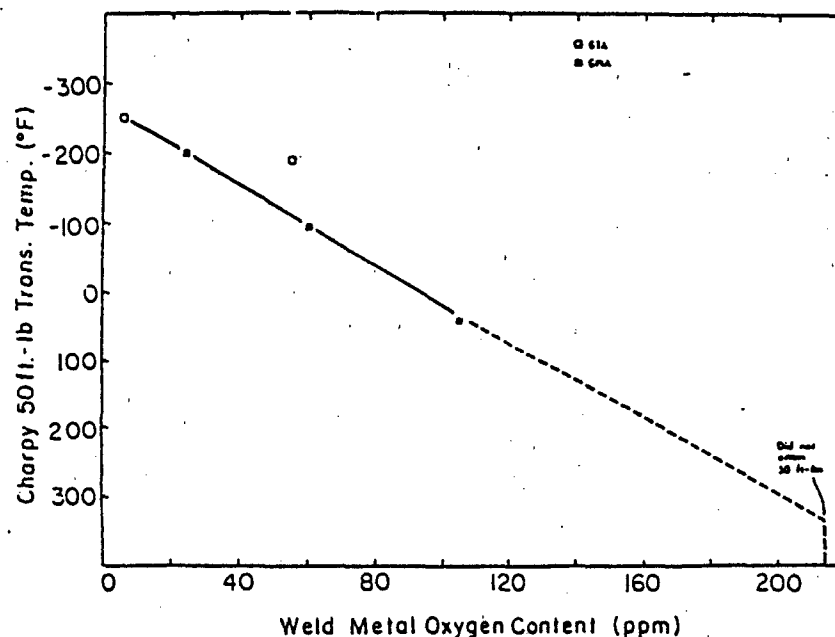


Figure 4. Effect of oxygen on the Charpy V notch shelf energy absorption in a 3% nickel weld metal. (after Stout, et al; [Ref. 8])

Nitrogen showed a similar effect in increasing the transition temperature. Both gases also had an effect on the strength level. [Ref. 3]

- **Titanium**

The role of Titanium is primarily to protect boron from nitrogen and oxygen and reduce the level of free nitrogen in the weld metal, resulting in an improved resistance against strain aging [Ref. 9]. Boron additions via  $B_2O_3$  in the flux are often performed so boron can retard ferrite growth.

The precipitation of TiN or titanium-bearing oxides permits boron to segregate to the prior austenite grain boundaries due to the suppression of boron compound precipitation. The boron segregation to austenite grain boundaries lowers the surface energy of the grain boundary and retards the nucleation of grain boundary ferrite. These titanium-bearing precipitates serve as nucleation sites for acicular ferrite at inclusions by entering deoxidation products. The best impact properties for IISLA steel are obtained when Ti is present to tie-up all free nitrogen in precipitates [Ref. 10].

## 2. Structure-Property Relationships in Bainitic Steels

Bainitic microstructures can arise in commercial steels by design of the alloy composition by proper processing or during welding operations. Bainitic steels can be improved by optimization of alloy chemistry and processing.

A recent development has been the use of accelerated cooling or direct quenching to achieve levels of mechanical properties characteristic of expensive heat-treated alloy steels from comparatively alloy-free compositions [Ref. 11].

The major advantage of processing steels in this way is that the weldability can be improved significantly by lowering the carbon equivalent value (CEV). The fracture toughness of bainite microstructures is a "local brittle zone" in the HAZ. The control of microstructures is of importance by alloying elements or controlling inclusions of the microstructure. (Cochrane et al., 1990, p.1527)

A description of bainite morphology is lath or plate shaped ferrite grains associated with carbide particles. Some morphological attributes do vary systematically with transformation temperature. These are lath size, lath shape, and carbide size and distribution. The latter forms the principal means of differentiating between "upper" and "lower" bainite. Upper bainite forms at relatively high transformation temperatures with carbides between ferrite laths, while lower bainite forms at lower temperatures and the carbides are contained entirely within the ferrite. There are often some differences in the ferrite morphology between the two types, although these may not be obvious on optical examination in low carbon steels (less than 0.15 weight percent carbon); the ferrite characteristic of upper bainite is lathlike, whereas in lower bainite, particularly in higher carbon steels, the ferrite grains are often platelike. (Cochrane et al., 1990, p.1528)

Another term commonly used to describe low-carbon bainitic steels is "acicular ferrite". This microstructure, particularly for low-carbon microalloyed Mn-Mo-Nb thermomechanically processed steels. This term is also, used to define the characteristic structures noted in as-deposited weld metals, and some guidelines are clearly possible and necessary so that an appropriate nomenclature can be used. The genesis of term "acicular ferrite" can be traced to early stages of the transformation behavior which showed that the steels formed transformation from a coarse-grain austenite. Studies using deformation dilatometry indicated that under controlled rolling conditions, a polygonal ferrite microstructure would be promoted. Close examination of such structures often shows them to consist of a number of "phases", and there is very little clear evidence of the the shelf/lath structure characteristic of bainite. (Cochrane et al., 1990, p.1529)

The similarity among Widmastatten ferrite, bainite, and martensite makes identification very difficult and it is often possible that several structure-property relationships may not be attributable solely to bainite on the basis of metallographic characteristics. It is also probable that various forms of truly acicular ferrite are variants of bainite and further detailed studies of the transformation kinetics should be encouraged for identification. (Cochrane et al., 1990, p.1530)

There are several methods of raising toughness: First by, processing the steel to achieve a fine austenite grain size, or by promoting a subdivision of the parent austenite by an bainite reaction. These methods require a fully bainitic microstructure from a fine austenite microstructure requires appreciable additions of alloying elements to maintain hardenability, whereas the idea of promoting bainite nucleation in a coarse-grained austenite, can be applied to low-alloyed steels. (Cochrane et al., 1990, p.1533) This could be further extended so that the limiting factor for cleavage is the lath size.

There is a critical range in weld metal oxygen content for optimum toughness, as a result proportions of coarse bainite or proeutectoid ferrite and the interlocking acicular ferrite intragranular bainite will determine the overall toughness of the weld (Cochrane et al., 1990, p.1537).

### 3. Inclusions in Steel

By decreasing the amount of oxygen and sulphur in the steel, one can decrease the effects of the inclusions on mechanical properties. The Electroslag Remelt (ESR) technique generally have low inclusions levels. This is because oxide inclusions go into solution in the molten tip during remelting. In Vacuum Remelt (VAR) steels have a greater freedom from oxide inclusions while ESR steels have more freedom from sulfides. The minimum oxygen level in VAR steel is limited by melt-refractory interactions and not oxygen content in the vacuum. (Kiessling and Lange, 1978, pp.24-25)

Non-metallic inclusions of steels fall into two groups, those of indigenous and those of exogenous origin. The former group contains inclusions occurring as a result of reactions taking place in the molten or solidifying steel bath, whereas the latter contains those resulting from mechanical incorporation of slags, refractories or other materials with which the molten steel comes in contact. The indigenous inclusions, are those that form by precipitation as a result of homogenous reactions in the steel. They are composed principally of oxides and sulphides and the reactions that form them may be induced either by additions to steel by changes in solubility during the cooling and freezing of the steel. Exogenous inclusions occur in a great variety but, for the most part, are readily distinguished from the indigenous inclusion. Characteristic features of exogenous inclusions include a generally larger size, sporadic occurrence, proffered location in ingot or casting, irregular shapes and complex structure. They are usually composed of oxides, a result of compositions of potential exogenous materials such as slags and refractories. (Kiessling and Lange, 1978, Part III p.1)

#### *a. Composition of Inclusions in Steel*

$\text{MnO-SiO}_2\text{-Al}_2\text{O}_3$  are indigenous oxide inclusions in modern steels. This system is of fundamental importance in steelmaking and serves as a convenient basis for the oxide systems present in non-metallic inclusions. The most important of these other systems are  $\text{MgO-SiO}_2\text{-Al}_2\text{O}_3$  and  $\text{CaO-SiO}_2\text{-Al}_2\text{O}_3$ , both are of special relevance to exogenous inclusions in steel. After oxygen, sulphur is the most important non-metallic element in steelmaking practice. [Ref. 12]

Oxides in our steels which are aluminum killed and treated with calcium are based on various calcium aluminates eg.  $(\text{CaOAl}_2\text{O}_3, \text{CaO}2\text{Al}_2\text{O}_3)$  which are molten during steelmaking and readily float to give clean steel. Mn and Si are not as strong deoxidants as Ca and Al so,  $\text{CaO}$  and  $\text{Al}_2\text{O}_3$  rich phases are formed.  $\text{CaO}$  has one of the lowest free energies of formation among common materials used to refine steel. Calcium has an high affinity for oxygen and is very effective deoxidant.  $\text{CaO}$  is usually called lime and is the cover slag material formed in basic steel processes.

Inclusions containing  $\text{MgO}$  are characterized by an exogenous origin, the main sources being refractories and the furnace or ladle slags. The  $\text{MgO}$  particle acts as a nucleation point for  $\text{CaO}$ ,  $\text{Al}_2\text{O}_3$  and  $\text{FeO}$ . These oxides may dissolve in the aluminate phases in steel inclusions, which may also dissolve oxides of titanium to form  $\text{TiO}$ , if the steel is Ti balanced. (Kiessling and Lange, 1978, p.40-41)

Kiessling and Lange have formed conclusions for the formation of the different sulfide types.  $\text{MnS}$  if type 1 is formed in rimmed or semi-killed steel. Where the oxygen content of the liquid steel is high and the sulfur solubility low, resulting in a precipitation of sulfide is parallel to the deoxidation process and oxygen are precipitated at the same time from the liquid steel. In alloyed steel the high alloy components may be present in the inclusions in solid solution in the sulfide phase and also as precipitated oxide phases. For example,  $(\text{MnCr})\text{S}$  and  $\text{MnOCr}_2\text{O}_3$ . Type 1 are irregular, often angular in shape and randomly distribute in steel. They usually are present in multiphase inclusions. (Kiessling and Lange, 1978, p.125)

Type II is found in killed steels, thoroughly deoxidized with Al, but without excess and where the oxygen content is low. These steels have a high sulfur solubility and the sulfide phase precipitates late in the last parts of the steel ingot to solidify. Type II sulfide is found in the primary grain boundaries in a dendritic, eutectic pattern.  $\text{Al}_2\text{O}_3$  is formed by the Al-deoxidant, and therefore corundum often acts as a nucleus for the sulfide phase or if found mixed with the sulfide, but always as a separate phase. The precipitation pattern for Type II sulfide depends more on temperature and oxygen con-

tent of the steel than for Type I sulfides, which are precipitated at higher temperatures and oxygen content. (Kiessling and Lange, 1978, pp.125-126)

Type III is found in steel which have been deoxidized with excess Al. It was earlier thought that the morphology of Type III sulfides was influenced by  $Al_2S_3$  or  $Al_2O_3$  nuclei. Kiessling, Bergh and Lange, studied the Al-content of the different sulfides types and found that no Al was present in solid solution in any of the sulfides, at least in amounts detectable with electron probe analysis greater than 0.1 weight percent. The nuclei of the  $Al_2O_3$ , which are associated with Type III sulfides are always present in separate phase and have no influence on the outer form of the sulfide. Type III are irregular often angular in shape and randomly distributed in the steel and always forms monophase inclusions. In the HY steels analyzed they were primarily Type III inclusions. (Kiessling and Lange, 1978, pp.125-126)

HY-80 is a Aluminum killed steel, and therefore the oxide inclusions expected to occur are those containing CaO,  $Al_2O_3$ , and some  $TiO_2$ , or TiN if the steel is balanced with Ti. SiO<sub>2</sub> and MnO inclusions only occur when Al contents are significantly below 0.01 weight percent. The sulfur contents are generally very low in HY-80 and so the sulfide inclusions are likely to be MnS Type III and/or Ca(Mn)S complexes.

#### *b. Relationship between Inclusions and Microstructure*

Utilizing a Particle Analyzing Scanning Electron Microscope, Pargeter et al determined the inclusion types and associated microstructural morphology with inclusion types. Acicular ferrite often appeared with aluminum bearing inclusions. Ferrite sideplates and grain boundary ferrite are often associated with silicon and manganese, with or without sulfur. Rare-earth metal (REM) oxides and boron nitrides also been reported to nucleate ferrite by other authors. [Ref. 13]

### **B. HY-80 WELD METAL**

#### **1. The Microstructure of HY-80 Steel Welds**

The toughness of the weld metal is significantly effected by its microstructure. The final weld metal microstructure will depend on complex variables such as [Ref. 9]:

- The total alloy content
- The concentration, chemical composition, and size distribution of non-metallic inclusions
- The solidification microstructure
- The prior austenite grain size
- The weld thermal cycle

On cooling of the weld metal, equiaxed ferrite grains nucleate and grow from prior austenite grain boundaries (grain boundary ferrite). Finally, carbon-enriched regions between acicular ferrite laths, or adjacent to grain boundary ferrite, may either transform to ferrite and carbide aggregates or martensite, or may remain, untransformed, as retained austenite (microphases) [Ref. 14].

The microstructures are fairly complex and that many details are not resolvable with light microscopy. While the microstructures do consist mainly of lower bainite, tempered and untempered martensite can also be present, especially at faster cooling rates. At slower cooling rates some acicular ferrite or blocky ferrite may form. Using transmission electron microscopy, small amounts of retained austenite were identified. The presence of a wide variety of structures can be contributed to segregation resulting from solidification. [Ref. 14].

## **2. Cooling Rate and Microstructure**

Cooling rate is one of the most important factors in determining the microstructure and properties of a metal. Figure 5 on page 15 [Ref. 15] shows the effect of cooling rate on the yield strength of gas metal arc and shielded metal arc deposits in HY-130. The yield strength drops off at the slower cooling rates while increasing for higher cooling rates.



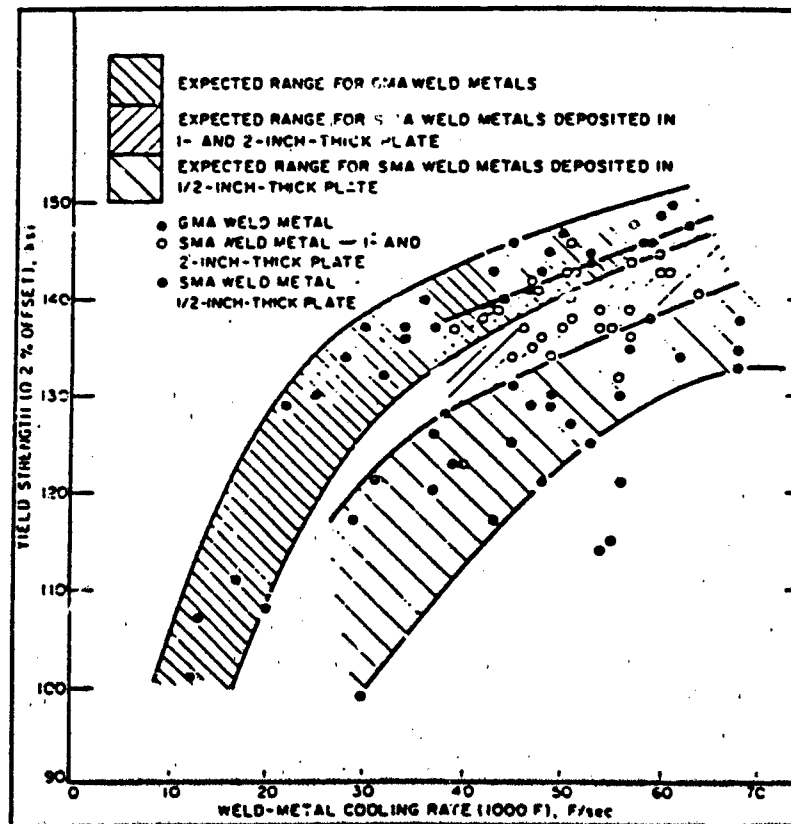


Figure 5. The effect of cooling rate on yield strength for GMAW and SMAW (Gross, et al; 1966, p.44)

For the best balance between strength and toughness, the cooling rate must be controlled within narrow limits. [Ref. 3]

The cooling rate of a weld is determined by many factors including plate thickness, thermal conductivity, heat input, and preheat. Increasing plate thickness increases the heat sink and the cooling rate and, conversely, thinner plates can present problems in obtaining sufficiently rapid cooling rates. In most welding operations the cooling rate is determined by the heat input and preheat. In the initial development work of Dorsch and Lesnewich it was found necessary to provide some preheat to avoid martensitic cracking [Ref. 7]. This is the primary reason for preheat in HY Steel. [Ref. 3]

### **3. Influence of Titanium on Weld Metal Microstructure and Properties**

At low weld metal aluminum levels, titanium seems to play an active role in nucleation of acicular ferrite at inclusions by entering the deoxidation products. Figure 6 on page 17 shows that small additions of titanium greater than 0.0045 percent Ti to the weld metal are essential in order to produce large proportions of acicular ferrite (Grong and Matlock, 1986, p.44). However, a very high concentration of titanium greater than 0.05-0.10 percent Ti can lead to a deterioration in toughness. This is believed to be caused by precipitation of finely dispersed, coherent TiN particles in ferrite, which will overshadow the beneficial effect on the gross microstructure. There is an optimum range of titanium which will produce maximum toughness in weld metals which will depend on the chemical composition of the weld. Figure 6 on page 17 illustrates when Ti is added through the filler wire or the flux high volume fractions of acicular ferrite is achieved. (Grong and Matlock, 1986, pp. 44-45)

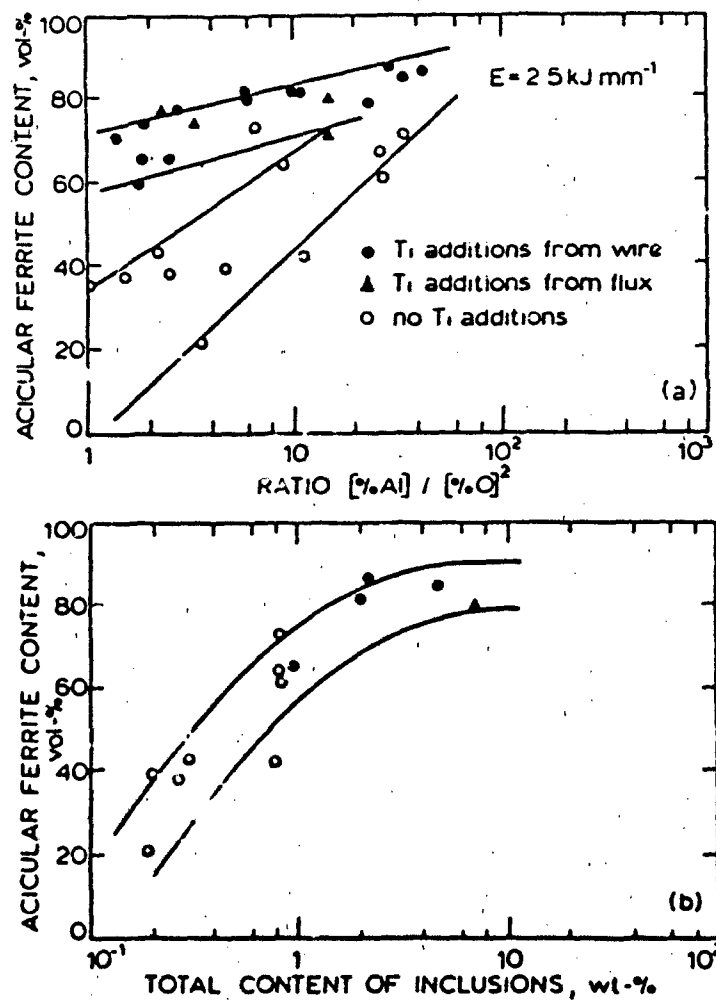


Figure 6. Role of Ti formation of acicular ferrite (Grong et al., 1986, p.44)

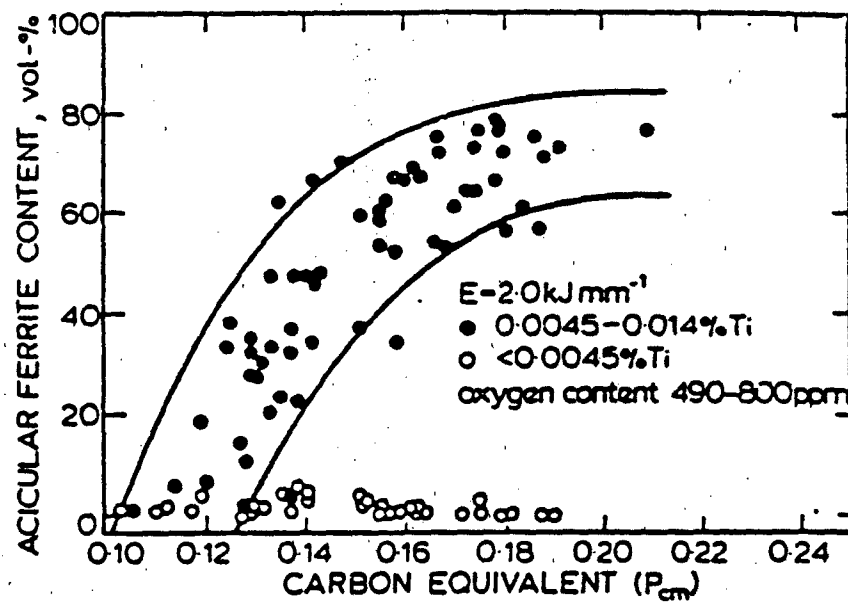


Figure 7. Effects of Ti on weld metal transformation (Grong et al., 1986, p.44)

Titanium often combines with nitrogen to form titanium nitride (TiN) or oxygen to form titanium oxide ( $TiO_2$ ). These particles are believed to reduce and control the uncombined oxygen level in the weld pool. TiN and  $TiO_2$  serve as nucleation sites for Ti, Mn, and Al oxides which form weld metal inclusions. Harrison and Farrar correlated oxide inclusion content level with the austenite grain size. A reduction in oxide inclusion developed large austenite grain size, implying that the inclusions may have an important effect on grain boundary pinning. [Ref. 16]

The recent improvements in weld metal toughness has been do to the understanding the ways to increase the volume fraction of acicular ferrite. By the additions of Boron usually with Ti one can eliminate coarse bainite due to boron pinning of grain boundaries which improves the toughness in the weld metal.

#### 4. Inclusions in Weld Metal

Inclusions commonly found in weldments will either be exogenous or indigenous, depending on their origin. The first type arises from entrapment of welding slags and surface scale, while indigenous inclusions are formed within the system as a result of deoxidation reactions (oxides) or solid state precipitation reactions (nitrides, carbides). The latter group is almost always seen to be heterogeneous in nature both with respect to chemistry (multiphase particles), shape (angular or spherical particles). (Grong et al., 1986, p.32)

Melting of the base metal and agitation within the weld pool results in dilution of filler with base material within the fusion zone. Impurities within the base material can react with alloying elements, perhaps forming inclusions of undesirable shape, or depleting elements. [Ref. 17]

Inclusions can also result from incomplete slag removal during multipass welding. Therefore slag detachability should be considered when multipass welding is to be performed. [Ref. 18]

The volume fraction and the total number on non-metallic inclusions in steel weld deposits is higher than normal in cast steel products, due to the limited time available for separation and growth of the particles. Also, the size of the inclusions are smaller and finely dispersed for the same reason. The average inclusion diameter is considerably larger in Submerged Arc (SA) welding compared with GMA for a given aluminum level as seen in Figure 8 on page 20.

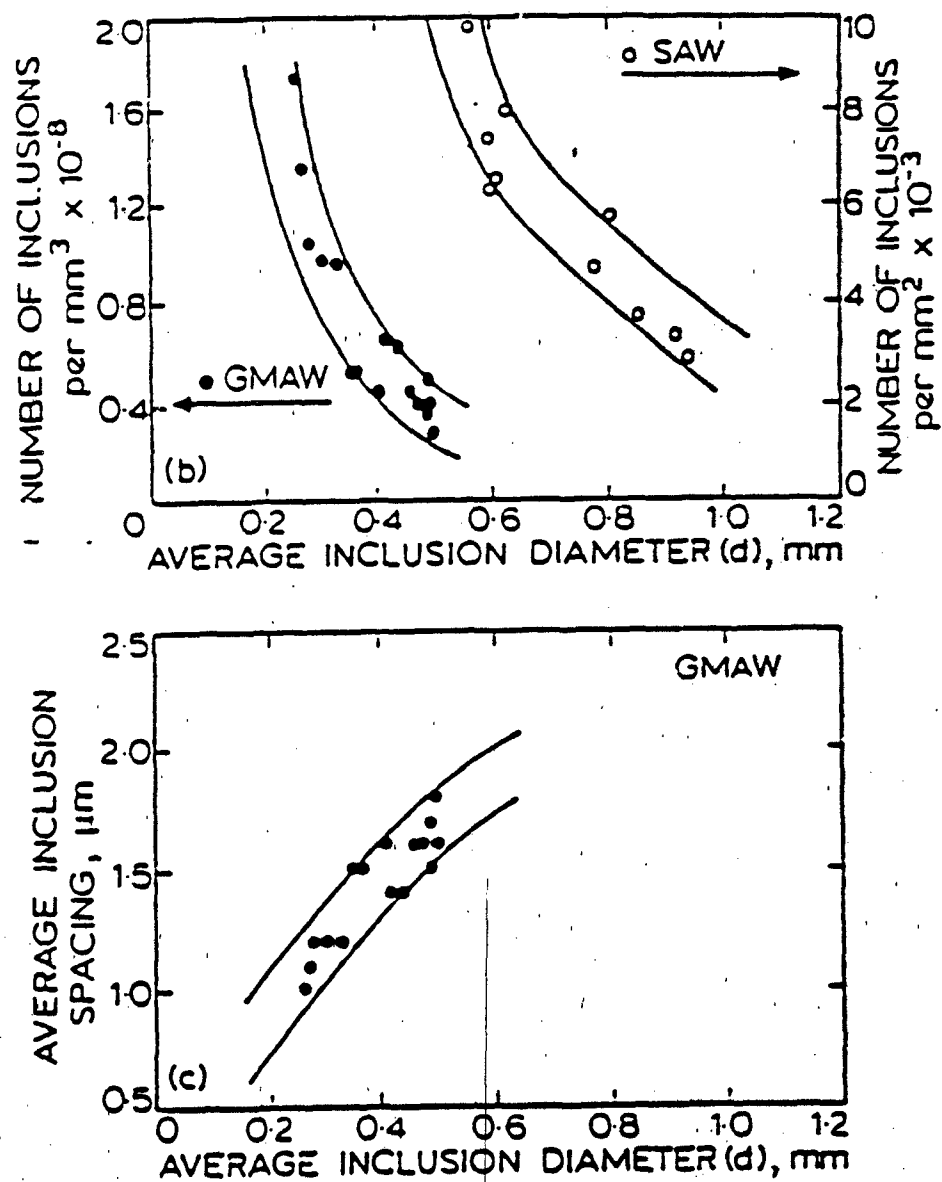


Figure 8. Size distribution of Non-metallic inclusions (Grong et al., 1986, p.33)

This difference is due to a higher heat input used in SA compared to GMA, which is found to promote growth of the particles because of the extended weld pool retention time (Grong et al., 1986, p.33).

The presence of inclusions affect the final properties of the weld metal. The weld metal prior austenite grain size, produced by variation in the density, volume fraction, and size distribution of inclusions can influence the mechanical properties of the weldment. In addition fine particles generally pin grain boundaries, restricting grain growth.

*a. Composition of Inclusions in Weld Metal*

Titanium is an alloying element which is of interest as a deoxidizer for steel. The free energy of formation is low for  $TiO_2$ . The coatings of welding electrodes are often rich in  $TiO_2$  and this coating forms a slag which is rich in titanium oxides. A study of the deoxidation mechanism of iron by titanium has been carried out by Evans and Sloman. A series of different titanium-iron-oxygen compounds were formed, which could be identified by X-ray diffraction methods. The phases arranged according to their increasing oxygen content, the following sequence of phases are found:  $TiO$ ,  $Ti_2O_3$ ,  $Ti_3O_5$ ,  $TiO_2$  (rutile),  $FeOTiO_3$  (ilmenite), and  $Fe_2TiO_4$  (inverse spinel) unknown phase called X-phase. The inclusions were further studied by Pickering, who identified microscopically all the phases except the  $Ti_3O_5$  and the X-phase. He questioned the identity of the  $TiO$  phase and suggested that this could also be  $TiN$ .  $TiN$  appears as a regular yellowish crystal usually at the grain boundaries. (Kiessling and Lange, 1978, p.125)

If titanium is present  $MnO-SiO_2-TiO_2$  inclusions are often found in silicon killed steels with less than 0.005 weight percent Al where as  $MnO-Al_2O_3-TiO_2$  inclusions are often found in lightly aluminum killed steels with 0.005-0.007 weight percent Al.

*b. Relationship between Inclusions and Microstructure*

The reduction in oxide inclusion content provides larger austenite grain structure, referring that these inclusions have an effect on grain-boundary pinning in weld metals. If titanium exists only as  $TiN$ , then the ternary phase diagram for  $Al_2O_3-MnO-SiO_2$ , as shown in Figure 9 on page 22 provides an indication of other phases which may occur.

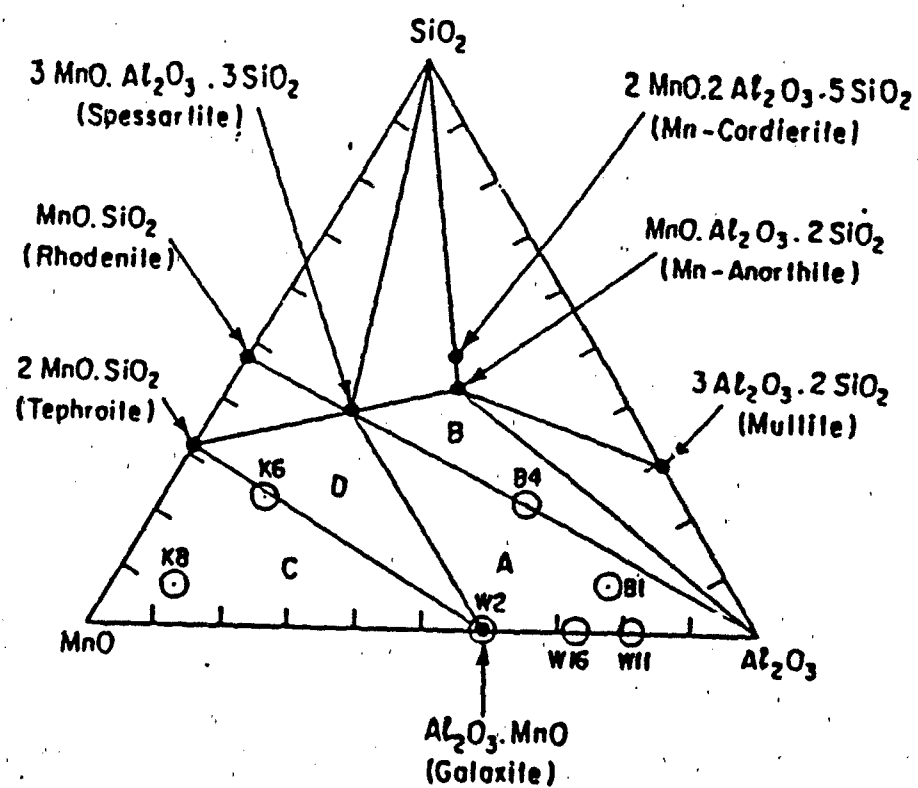


Figure 9. Ternary phase diagram for  $Al_2O_3$ -MnO-SiO<sub>2</sub> (Corbett et al., 1985, p.1619)



Because equilibrium is not reached in molten welds, the equilibrium phase show in Figure 9 may not form. In addition weld inclusions contained titanium and therefore  $Al_2O_3$ - $TiO_2$ -MnO or  $Al_2O_3$ - $TiO_2$ -MnO- $SiO_2$  diagram might be more appropriate. However,  $Al_2O_3$  may not be present if Al level in weld metal is low. Despite extensive searches in the literature, no such phase diagrams have been found. (Corbett et al., 1985, pp.1618-1619)

### C. WELDING PROCESS

A reduction in hull fabrication costs and higher productivity can be achieved by substitution of an HSLA steel for HY Steel. The significant factor in cost savings through the use of HSLA steel is the elimination or reduction of preheat for welding. The most important property in evaluating the quality of high strength steel weld produced by the GMAW process is the fracture toughness of the weld metal. This is strongly influenced by controlling the chemical composition and cooling rate of the weldment. The use of welding consumables results in some restrictions of welding process that must be closely controlled in order to optimize fracture toughness include (Potkay, 1987, p. 32):

- Voltage
- Current
- Travel Speed
- Arc Length
- Preheat/Interpass temperature
- Number of passes
- Electrode feed rate
- Consumable composition
- Joint Geometry

#### 1. The GMAW Process

A significant portion of the cost of ship construction is attributed to welding. The cost of ship construction has been substantially reduced by the cost effectiveness of automation and high deposition rates. Figure 10 on page 24 illustrates the GMAW process used in this investigation.

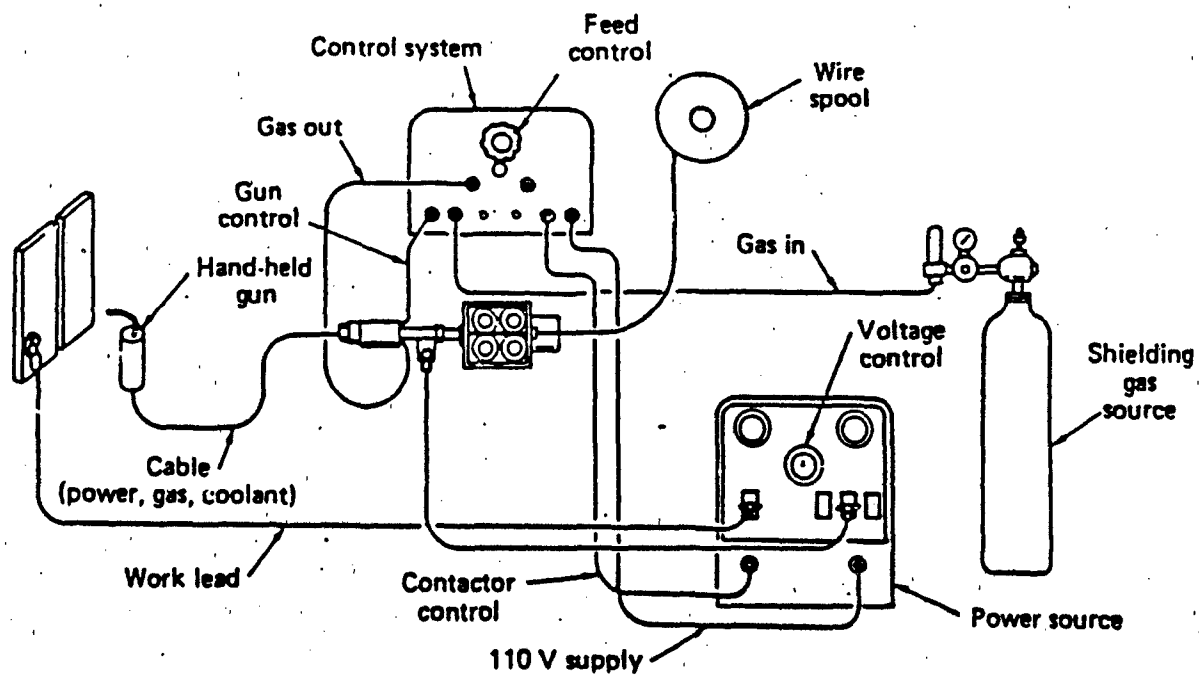


Figure 10. GMAW Process ([Ref. 19])

In this process the arc between the electrode and the workpiece melts to allow a fusion weld to form. The welding heat is obtained from an arc between a consumable electrode and the workpiece. Oxygen is deliberately introduced through the shielding gas to improve arc stability. A major variation of the GMAW process is the flux-core arc welding where fluxes can be incorporated into the GMAW process. The composition of the filler material used in this experiment are show in Table 2.

**Table 2. CHEMICAL COMPOSITION OF FILLER MATERIAL MIL-100S,**  
(values in weight percent either maximum value or range) yield stress  
82-110ksi, elongation 16 percent.

ELEMENT	MIL-100S
C	0.08
Mn	0.08
Si	0.2-0.55
P	0.01
S	0.01
Ni	1.4-2.1
Mo	0.25-0.55
Cr	0.30
V	0.05
Al	0.10
Ti	0.10
Zr	0.10

The gas metal arc process offers the advantages of high deposition rates and relatively clean deposited weld metal. Since there is no flux, moisture pickup is limited to the surfaces of the filler wire and the base plate. The main disadvantage is the loss of shielding gas, in windy conditions and position limitations in some cases. Normally argon, helium or a mixture of both are used as a shielding gas to protect the weld zone. Direct current reverse polarity (DCRP) process is primarily used due to higher deposition rates that are required.

Inclusions are formed at temperatures about 1800 C and are trapped in the metal. The final concentrations of oxygen, silicon, titanium and manganese in GMA weld deposits are controlled by reactions in the small volume of stirred hot metal immediately beneath the root of the arc. (Grong and Matlock, 1986, p.32)

#### **D. HY-80 HAZ MICROSTRUCTURE**

Examination with the Transmission Electron Microscopy (TEM) of the HAZ revealed a microstructure of tempered martensite and tempered bainite with a uniform distribution of cementite.

Chen and Thompson [Ref. 20] conducted a study on HY-130 weldments, concentrating on the HAZ for examination with the transmission electron microscope. The predominate microstructures observed were martensite and bainite, in a variety of forms and sizes. Retained austenite was found in several areas, although it was present in relatively small amounts when compared to the predominantly martensitic and bainitic structure. This retained austenite was found only in the GMAW welds, but the factors underlying the result were not explained. Carbides were found in a number of the microstructures and the morphology of the carbides was found to be similar to those seen in lower bainite (elongated rods). Diffraction information from the carbides was extremely faint and, therefore, conclusive identification was not made. [Ref. 21]

##### **1. Influence of Titanium on HAZ Microstructure**

Nitrogen has a severe effect on the deposited weld metal; first by causing porosity, and secondly by embrittlement. Ti can neutralize the negative impurity effects of nitrogen present in the HAZ.

Titanium nitride may have two effects. First, it enhances intragranular ferrite nucleation producing an acicular ferrite structure with improved toughness. Secondly, it is a grain growth inhibitor. Optimum austenite boundary pinning is obtained with TiN particle size less than 0.05  $\mu\text{m}$ , and a titanium content of about 0.015 percent. [Ref. 22] It has been suggested that Ti up to additions of about 0.04 weight percent have been found to produce a small increase in acicular ferrite which has a beneficial effect on toughness by refinement in microstructure. [Ref. 23]

There are coarse grains in the HAZ near the weld pool resulting in low toughness. In the coarse grain HAZ where re-austenitization occurs several times in a multipass weld Ti appears to keep the grain size smaller here and increases the toughness.

#### **E. SCOPE OF PRESENT WORK**

The purpose of the thesis is to examine HY-80 multipass weldments treated with Ti and untreated with respect to non-metallic inclusions and their effect on microstructure. Information regarding the size, distribution and composition will be gathered by use of a scanning electron microscope and Energy Dispersive X-Ray analysis (EDX). Trans-

mission Electron Microscopy (TEM) will be utilized to understand the improvements in HAZ, and parent metal multipass GMAW steels when small amounts of Ti are present. According to Farrar [Ref. 1] small additions of Ti to high strength steel weld metal improves its toughness and that the improvements are due to refinement in microstructure.

### III. EXPERIMENTAL PROCEDURE

#### A. MATERIAL

Two HY-80 steel samples one treated with Ti and one not were provided by the David Taylor Research Center (DTRC), Annapolis, Maryland. The welded samples were a multipass GMAW with a heat input of 100KJ/in and 167 C preheat. Both steels are Al killed and Ca treated. In the Ti treated steel Basic Oxygen Furnace (BOF) steelmaking process was used. In the BOF process, pure oxygen is introduced above the surface of the molten bath. This process is adopted to the process of a blast furnace and with medium to high phosphorus contents. In the non-Ti treated steel the Electric Arc Furnace (EAF) was utilized. The absence of an oxidizing heat source permits deoxidized products in the furnace not to be as rapidly reoxidized in the molten metal. The BOF process usually tends to produce cleaner steels with fewer non-metallic inclusions. The experimental procedures consisted of information regarding the size, distribution and composition of non-metallic inclusions in the HAZ, and parent metal.

#### B. MECHANICAL PROPERTIES

Charpy V-notch impact energy, for HY-80 GMA treated with Ti and without was conducted by Artech Corporation and data provided to the author by DTRC.

#### C. MICROSCOPY

##### 1. Optical Microscopy

Metallographic mounted and unmounted samples were cut and prepared so a plane parallel to the plane of the HAZ and parent metal could be photographed under optical and SEM magnification to document the general microstructure. Both samples were ground on successive emery paper to 600 grit and polished on a 6 $\mu$ m diamond wheel; then on a 1 $\mu$ m diamond wheel. Special care was taken not to over polish, which can result in removal of small inclusions or any contaminate in subsequent polishing. Specimens were ultrasonically cleaned in ethanol rinsed and blown dry. Mounted samples were etched for approximately 20 seconds using a 2 percent nital etching solution for overall microstructure analysis. The unmounted samples were etched for 1 minute with an aqueous picric etchant with sodium dodecylbenzenesulfonate added as a wetting agent for overall prior austenite grain size measurement.

#### **D. SCANNING ELECTRON MICROSCOPY**

Photographs of etched (Modified Winsteads) solution using Back Scatter (BS) and Secondary Electron (SE) image were taken for use in determining prior austenite grain size and for quantitative analysis on multiphase inclusions and microstructural features. Information about the composition size, and distribution of inclusions were gathered by use of a Cambridge Stero Scan S200 Scanning Electron Microscope and Energy Dispersive X-Ray Analysis (EDX). Chemical analysis of inclusions was conducted with the EDX Spectrometer.

#### **E. TRANSMISSION ELECTRON MICROSCOPY**

Wafered samples perpendicular to the plane of the deposited weld metal were prepared using a low speed diamond saw. Each wafer was hand sanded to a thickness of less than 0.05mm. The wafers were etched for 10 seconds in a 2 percent nital solution and optical examination was conducted to map out the weld, HAZ, and parent metal microstructure. Three-millimeter discs were punched out from the locations discussed above. Discs were electrochemically thinned to perforation in a Stuers Tenupol electropolishing device operating at 70 volts with a medium flow rate of 3 percent perchloric acid, 62 percent ethanol, and 35 percent n-Butoxy Ethanol solution, cooled to -35 C with liquid nitrogen.

TEM was utilized to characterize the microstructure on the HAZ, weld, and parent Ti treated metal on JEOL model JEM100CX operating at 120kV and a JEOL model 200CX operating at 200kV at the National Center for Electron Microscopy located at Lawrence Berkeley Laboratory, Berkeley, California.

## IV. RESULTS AND DISCUSSION

### A. MICROSTRUCTURAL OBSERVATION IN HAZ AND PARENT METAL

The HAZ and parent metal of Ti treated and non treated samples were examined with optical, SEM, and TEM microscopy. This investigation was conducted to characterize, the microstructure of the HAZ with a view to monitoring the possible pinning of the prior austenite grain boundaries by Ti inclusions.

### B. OPTICAL MICROSCOPY

Light microscopy did not give significant information on the size of the non-metallic inclusions as the sizes were often between  $0.5\mu\text{m}$ - $2\mu\text{m}$ . The majority of the small inclusions identified were near or at the limit of resolution of the microscope ( $0.2\mu\text{m}$  oil immersion). The literature reviewed indicated that the mean of the inclusion size distribution lies below this limit. However, TiN, MnS, and Oxide inclusions between  $4\mu\text{m}$ - $5\mu\text{m}$  in diameter were observed. A montage as shown in Figure 11 on page 31 of the deposited weld metal revealed the microstructural detail in the weld, HAZ, and parent metal.

### C. SCANNING ELECTRON MICROSCOPY

#### 1. SEM Microscopy

Microstructure observed by the SEM, revealed a bainite and martensite structure in the parent metal and in the HAZ a tempered bainite and tempered martensite microstructure. Micrographs were taken to measure the prior austenite grain boundaries. Micrographs were also, taken of Ti and multiphase inclusions to find out if non-metallic inclusions pinned austenite grains, and refined the lath structure, since small inclusions are effective in pinning austenite grain boundaries. Specific inclusions in the HAZ were micrographed at high magnification in attempt to see if TiN or  $\text{CaO-TiO}_2\text{-Al}_2\text{O}_3$  were pinning grain boundaries.

##### *a. Ti Treated HAZ Microstructure*

In Figure 12 on page 32 shows the Ti Treated HAZ average prior austenite grain size of approximately  $5\mu\text{m}$ .





**Figure 11.** Montage of Microstructure showing the weld pool, HAZ and parent metal

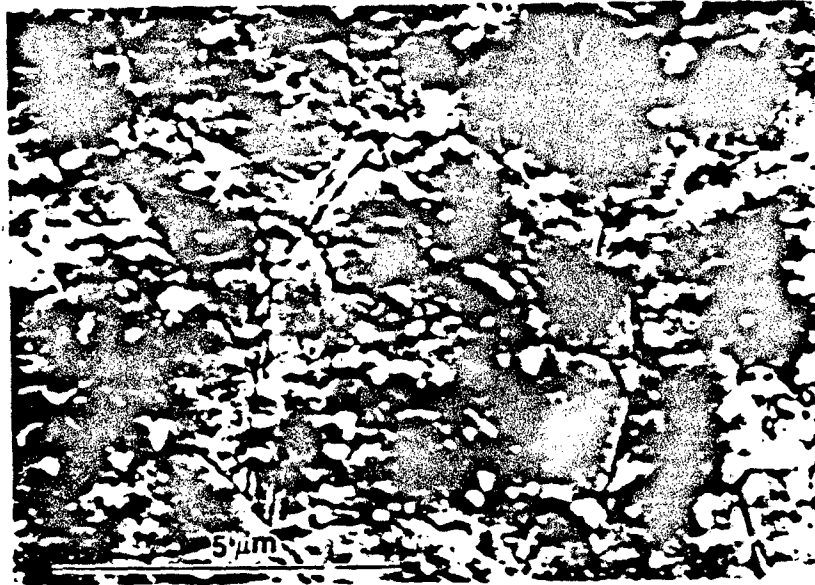


Figure 12. SEM Micrograph Ti Treated HAZ Prior Austenite Grain Boundaries  
SE Image, Etchant Modified Winsteads solution 1 minute

*b. Ti Treated Parent Metal Microstructure*

Figure 13 on page 33 , illustrates the bainite and martensite microstructure with  $TiO_2$  inclusion within the matrix.

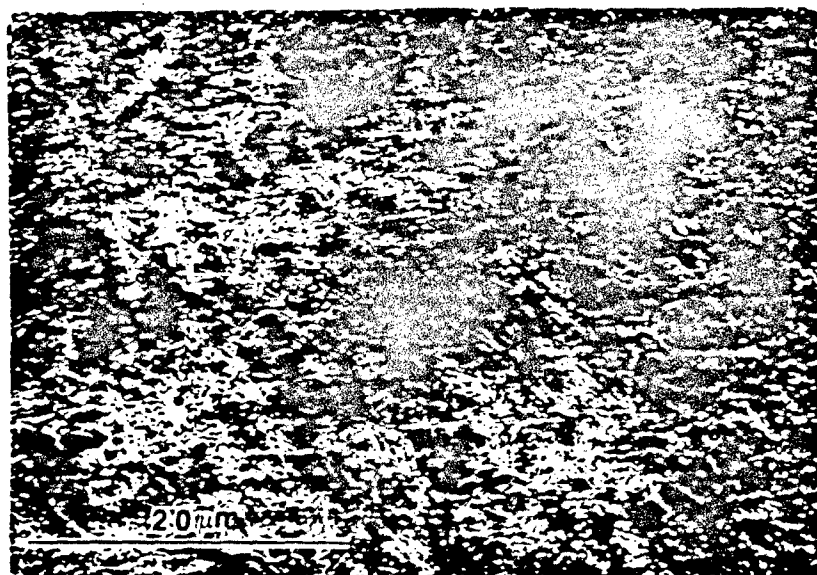


Figure 13. SEM Micrograph Ti Treated Parent Metal  $TiO_2$  inclusion SE Image, Etchant Modified Winsteads solution 1 minute

*c. Non-Ti Treated HAZ Microstructure*

Figure 14 on page 34 shows average prior austenite grain size of 8u for the non Ti treated HAZ.

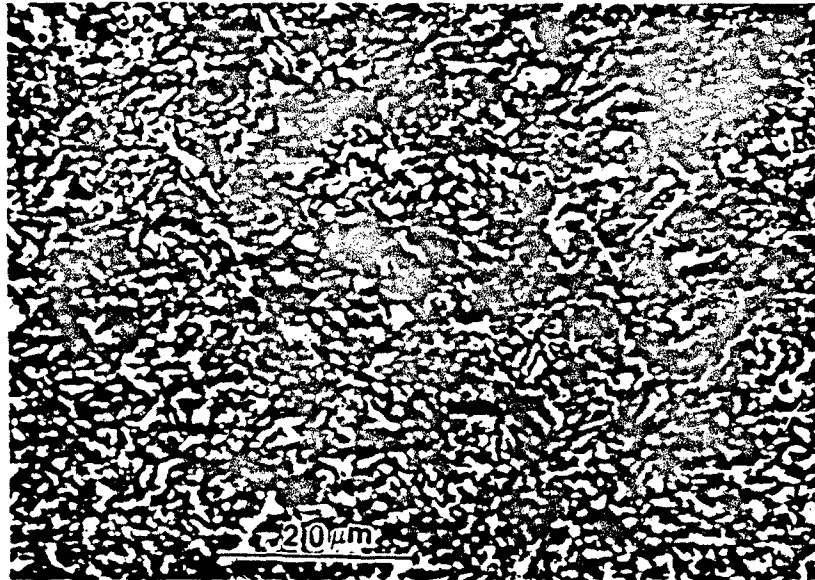


Figure 14. SEM Micrograph Non Ti Treated HAZ Grain Boundaries BSE Image,  
Etchant Modified Winsteards solution 1 minute

*d. Non-Ti Treated Parent Metal Microstructure*

In Figure 15 on page 35 reveals an average prior austenite grain size of 20μm for the non Ti treated parent metal.

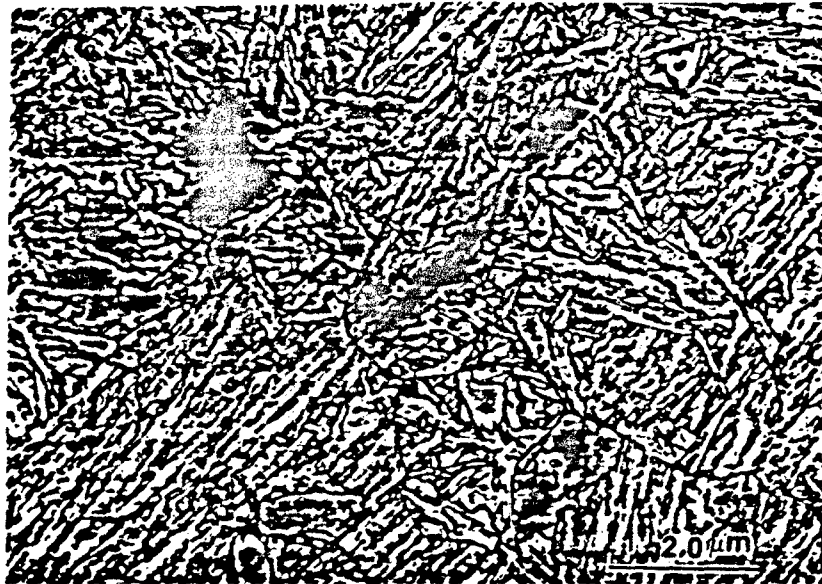


Figure 15. SEM Micrograph Non Ti Treated Parent Metal Grain Boundaries SE Image, Etchant Modified Winsteards solution 1 minute

*e. Ti Treated HAZ Inclusion Micrographs*

Figure 16 on page 36 illustrates a titanium oxide inclusion where Ti is neutralizing the negative effects of oxygen in the Ti treated HAZ.

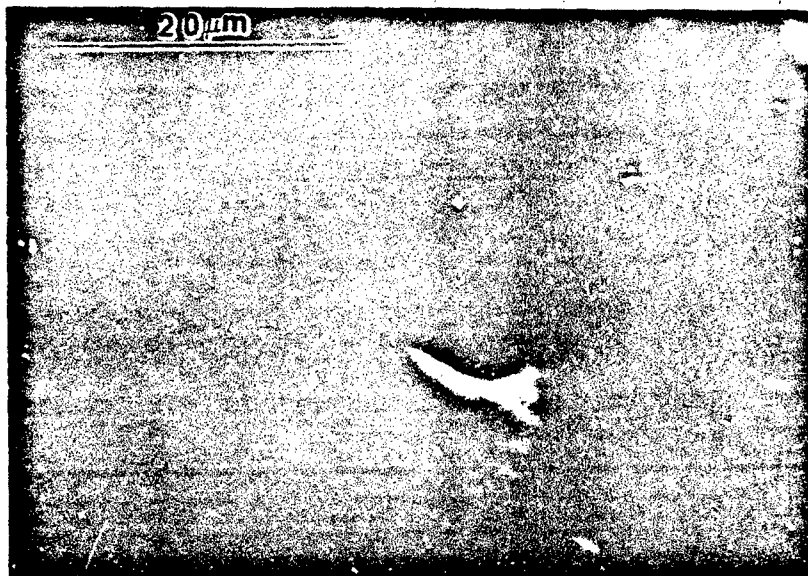


Figure 16. SEM Micrograph Ti Treated HAZ SE Image, Titanium Oxide inclusion Etchant Modified Winsteads solution 1 minute

Figure 17 on page 37 illustrates a  $\text{TiZrN}$  inclusion and a shaped modified  $\text{Ca(Mn)S}$ .  
(A on micrograph)

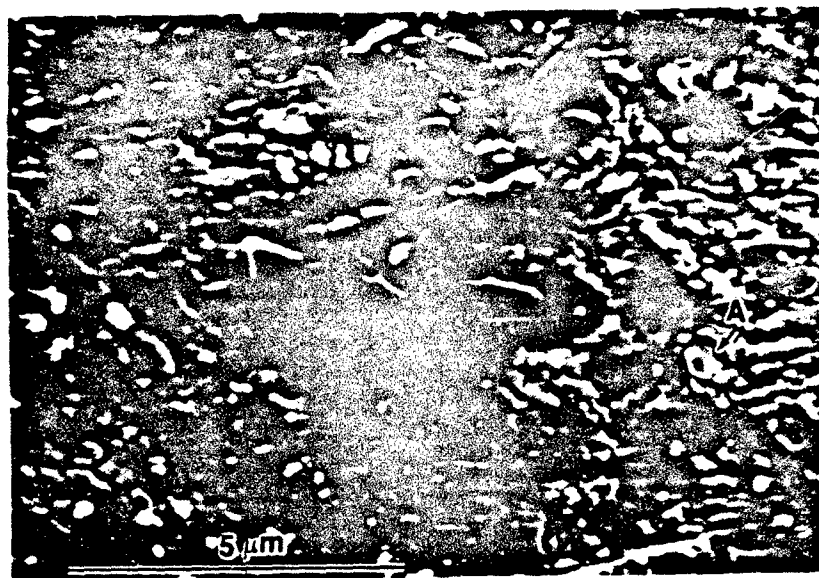


Figure 17. SEM Micrograph Ti Treated HAZ multiphase TiZrN inclusion and Ca(Mn)S inclusion BSE Image, Etchant Modified Winsteards solution 1 minute

The EDX analysis is shown in Figure 18 on page 38 for this inclusion.

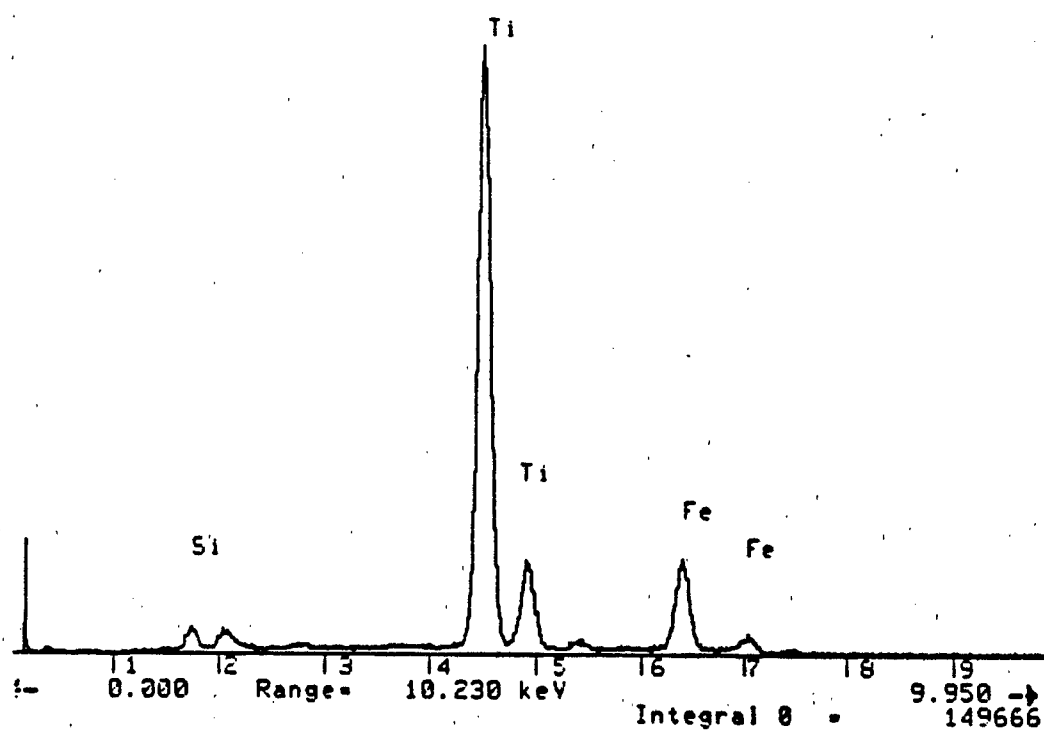
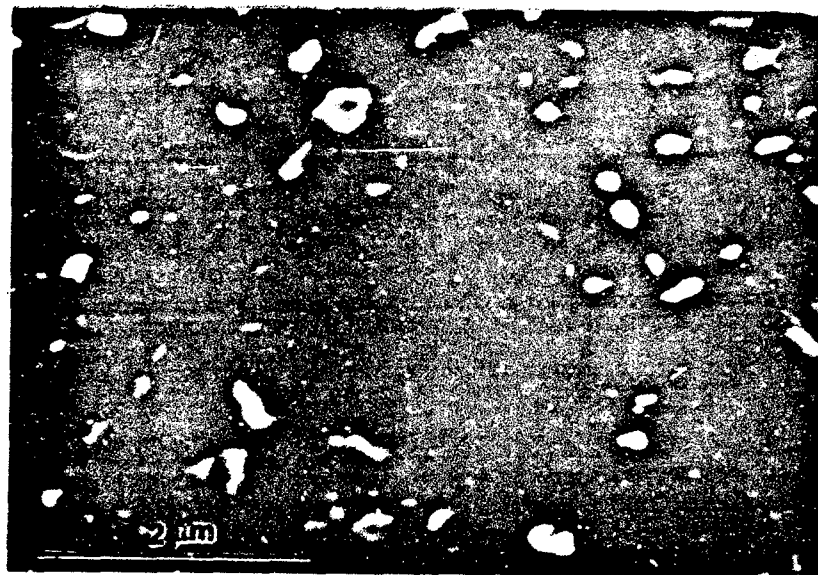


Figure 18. EDX Analysis multiphase TiZrN inclusion



Figure 19 on page 39 illustrates a multiphase Ti inclusion in the Ti treated HAZ. The EDX analysis for this particular inclusion is show in Figure 20 on page 40



**Figure 19. SEM Micrograph Ti Treated HAZ  $\text{CaAlTiMgO}$  inclusion BSE Image, Etchant Modified Winsteads solution 1 minute**

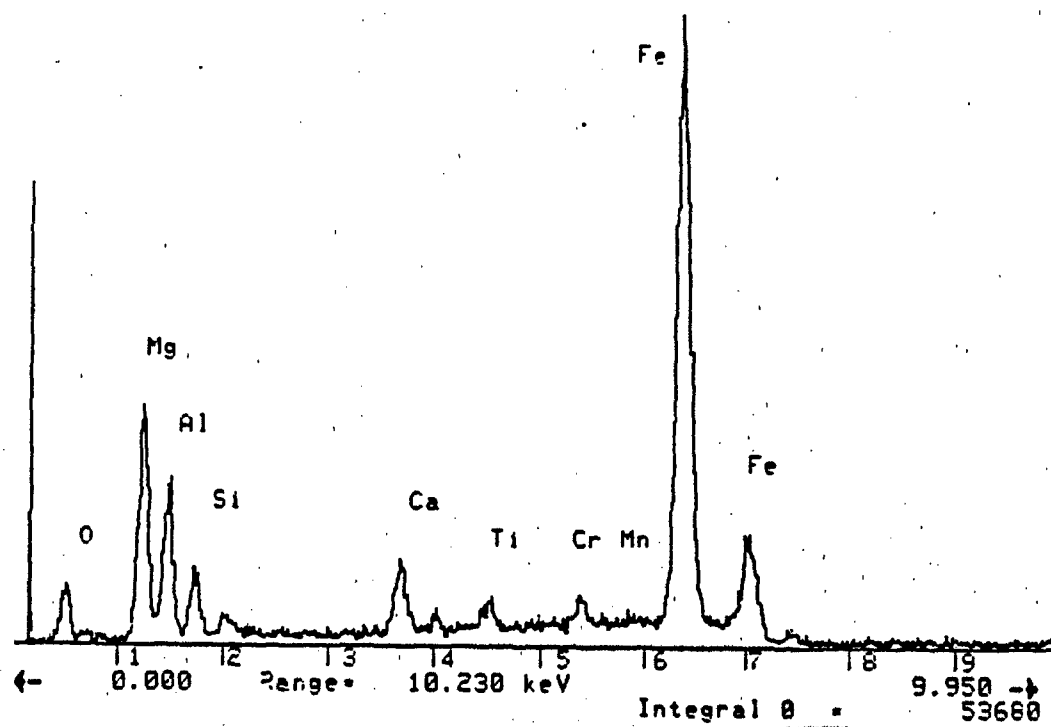
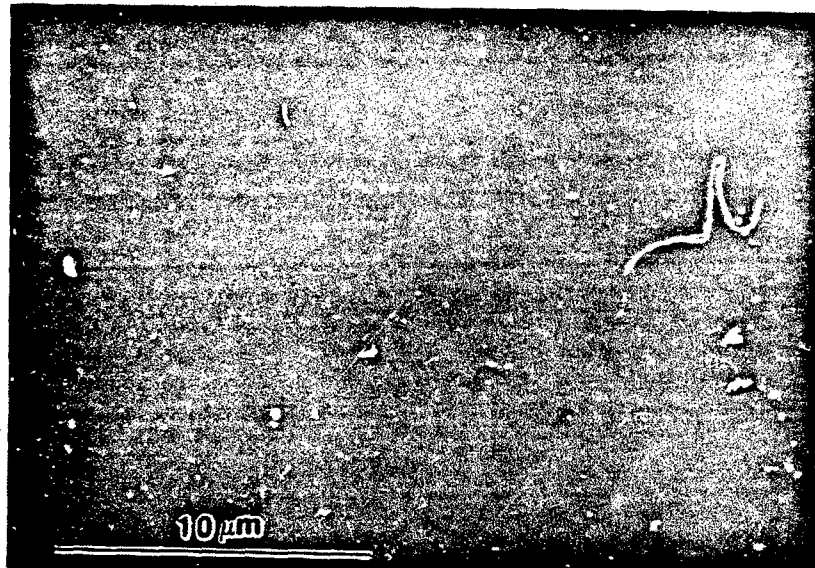


Figure 20. EDX Analysis multiphase CaAlTiMgO inclusion

*f. Ti Treated Parent Metal Inclusion Micrographs*

As shown in Figure 21 on page 41 a globular Type III MnS of  $4\mu\text{m}$  was observed in the Ti treated parent metal whereas in the untreated parent metal a larger globular Type III MnS of  $20\mu\text{m}$  was observed and micrographed refer to Figure 22 on page 42



**Figure 21. SEM Micrograph Ti Treated Parent Metal MnS Type III inclusion  
BSE Image**

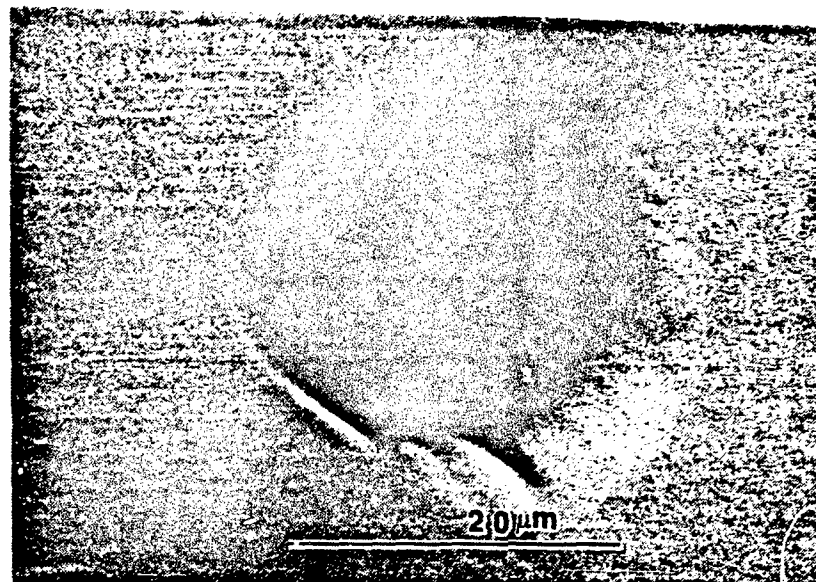


Figure 22. SEM Micrograph Non Ti Treated Parent Metal MnS Type III inclusion BSE Image, Etchant Modified Winsteards solution 1 minute

Figure 23 on page 43 illustrates a  $5\mu\text{m}$  TiN square inclusion and appears yellowish in color optically at the grain boundaries.

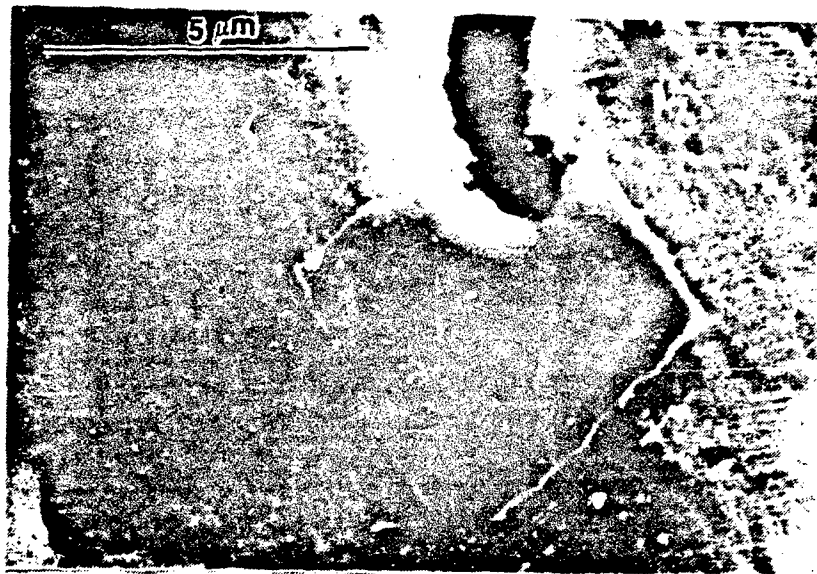


Figure 23. SEM Micrograph Ti Treated Parent Metal TiN inclusion SE Image,  
Etchant Modified Winsteards solution 1 minute

In Figure 24 on page 44 illustrates a 4μm TiN inclusion within the Ti treated Parent Metal.

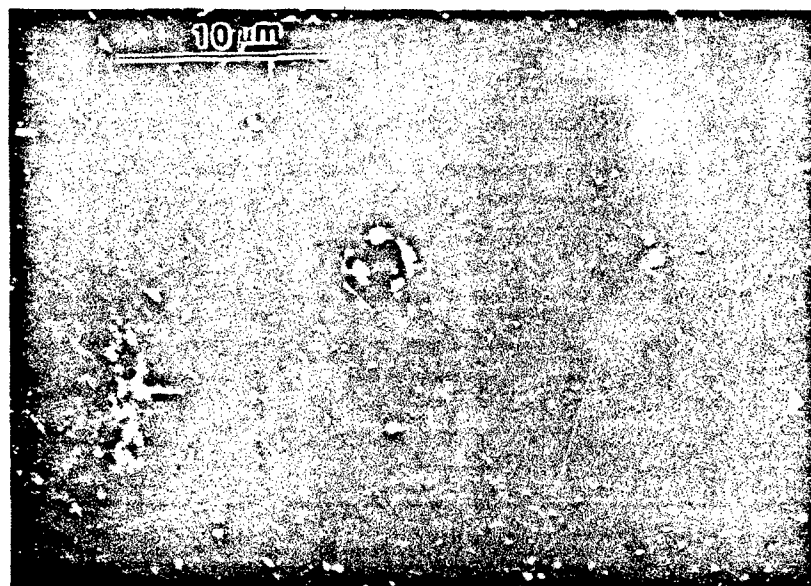


Figure 24. SEM Micrograph Ti Treated Parent Metal TiN inclusion SE Image, Etchant Modified Winsteards solution 1 minute

SEM micrographs of the parent metal and of the HAZ reveal a average prior austenite grain size of  $20\mu\text{m}$  and  $5\mu\text{m}$  for Ti treated and, for non Ti treated  $20\mu\text{m}$  and  $8\mu\text{m}$  respectively.

## 2. EDX Analysis

Evaluation of the non-metallic inclusions found in the weld, HAZ, and parent metal was achieved with the EDX/KEVEX analysis to determine the chemical nature of inclusions and the size distribution using 100 fields. The particles that were of sufficient size to analyze using EDX contained the following elements: aluminum, titanium, chromium, nickel, molybdenum, silicon, manganese, and iron. Inclusion size distributions for oxides, nitrides, and sulfides are presented are Figure 25 on page 46 , Figure 26 on page 47 , Figure 27 on page 48 and Figure 28 on page 49 for non Ti treated and the following Ti treated figures: Figure 29 on page 50 ,Figure 30 on page 51 , Figure 31 on page 52 , Figure 32 on page 53 , Figure 33 on page 54 , and Figure 34 on page 55 as bar graphs indicating the occurrence frequency as a function of lot size. From these results there is evidence, that Ti combines with Nitrogen or Oxygen to reduce the uncombined oxygen level and assists the calcium with sulfide shape modification. Large globular MnS inclusions were observed in the non Ti treated sam-

ples due to the high solidification rate in the weld pool. MnS inclusions within the HAZ contribute to hot-tearing phenomenon in welded steels (Kießling and Lange, 1980, p.101). The inclusion distribution influences the austenite to ferrite transformation one by providing nucleation sites for ferrite during transformation or by pinning the prior austenite grain boundaries.

# B-BASE PARENT METAL

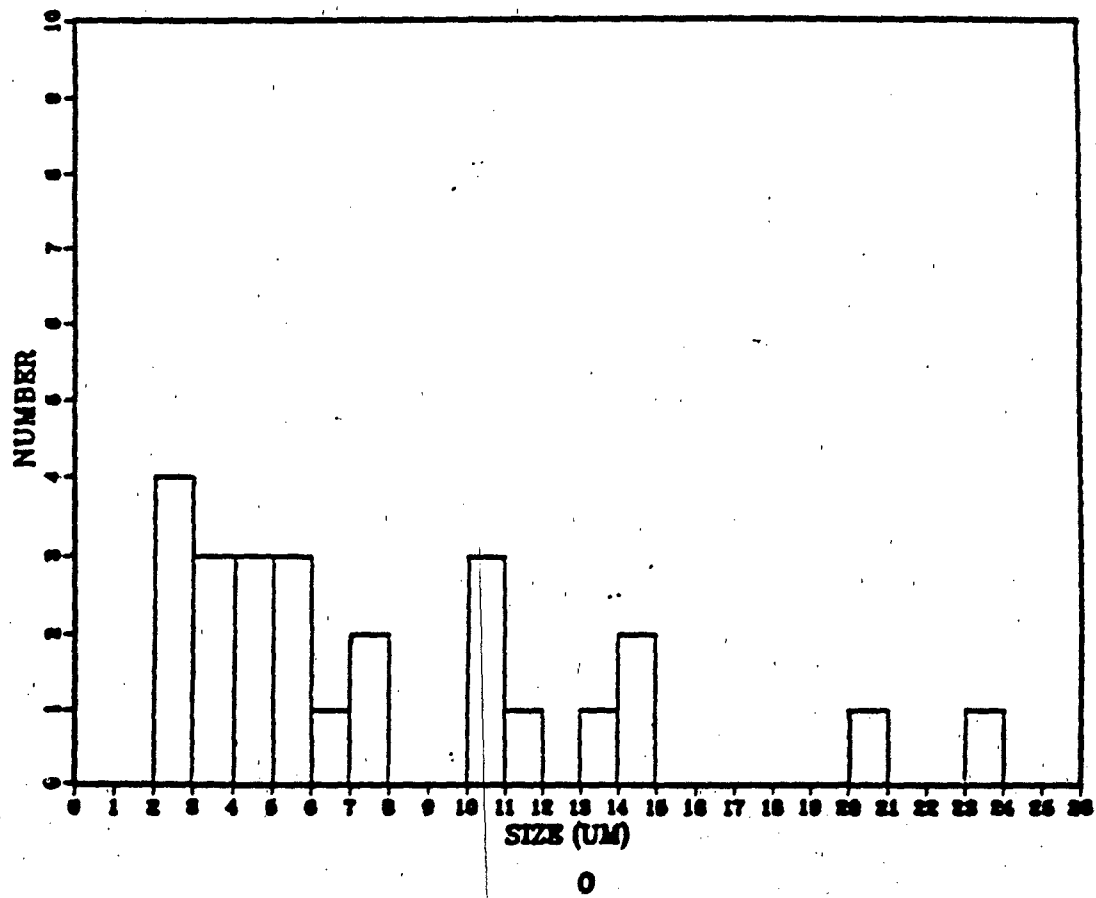


Figure 25. Oxide Inclusion distribution Non Ti Treated Parent Metal



# B-BASE PARENT METAL

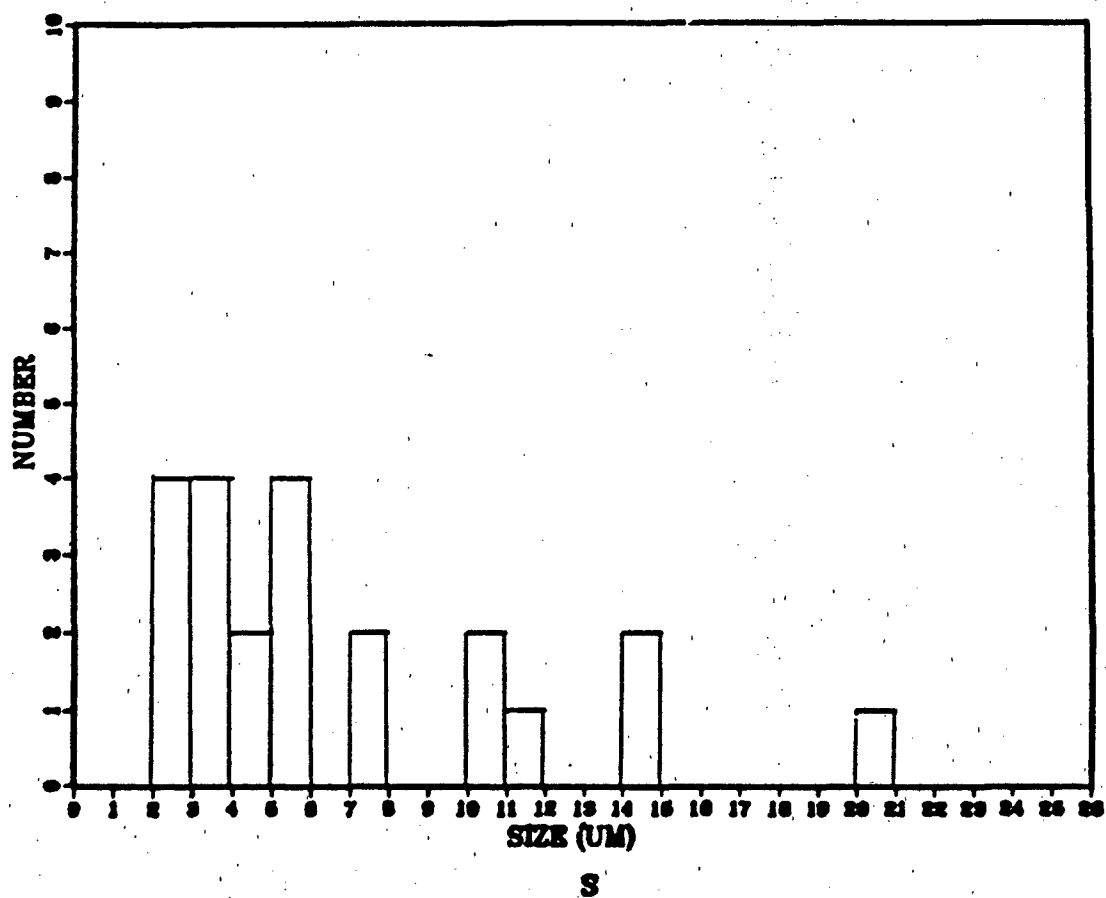


Figure 26. Sulfide Inclusion distribution Non Ti Treated Parent Metal

# B-BASE

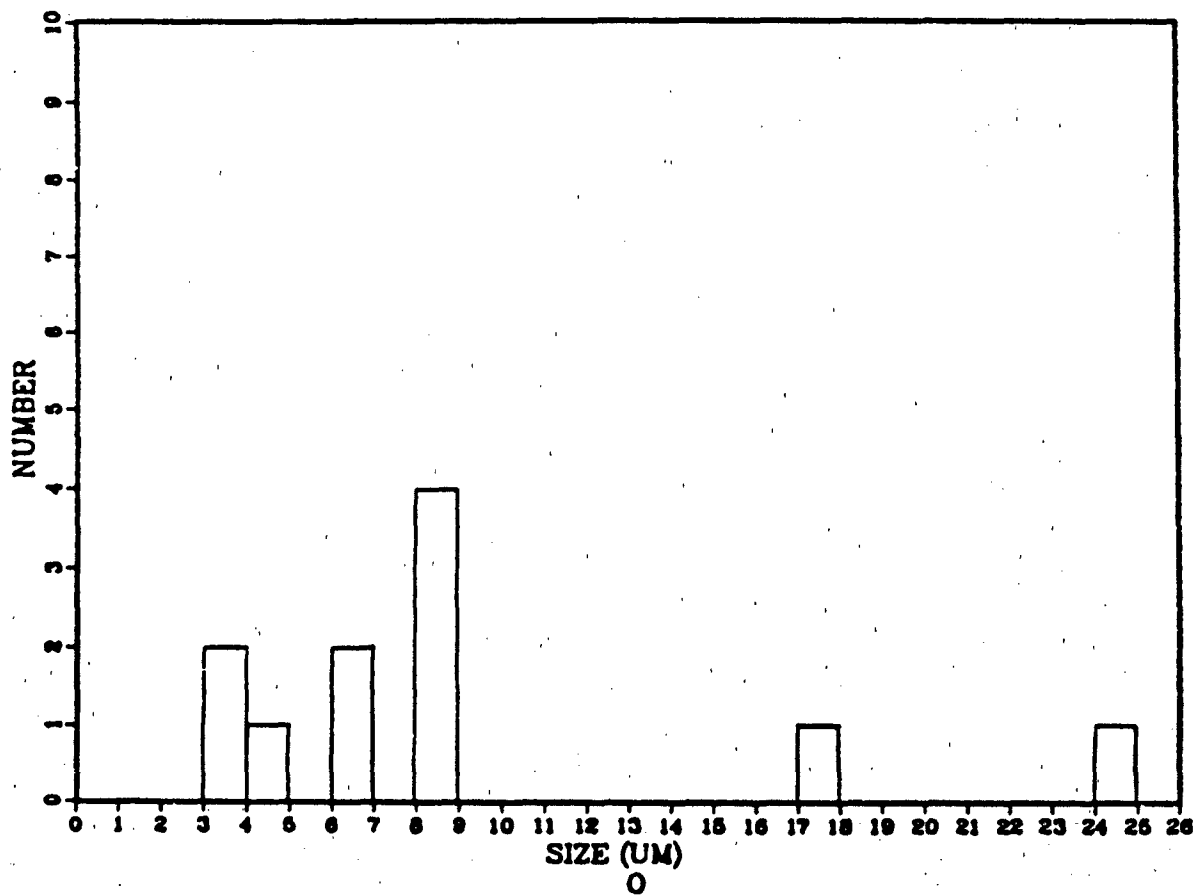


Figure 27. Oxide Inclusion distribution Non Ti Treated Parent, HAZ, Weld

# B-BASE

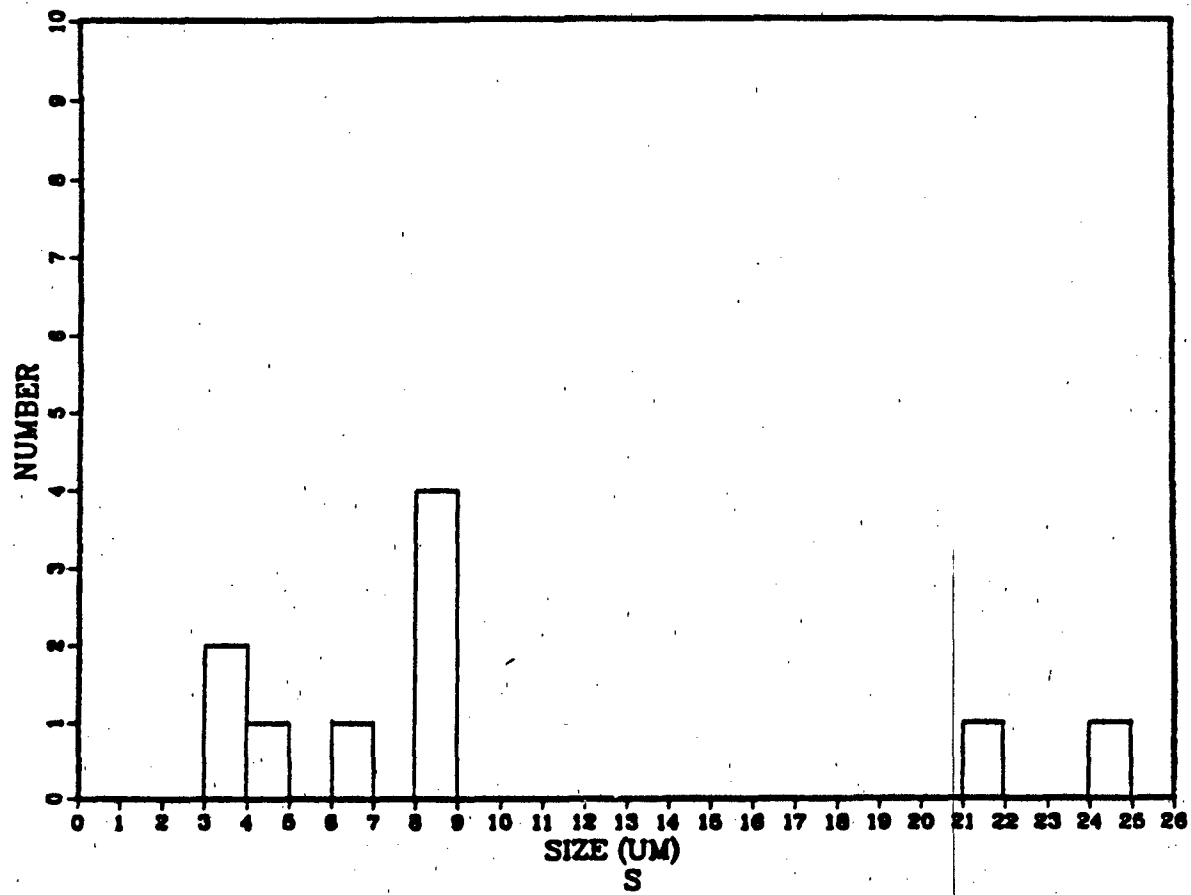


Figure 28. Sulfide Inclusion distribution Non TI Treated Parent, HAZ, Weld

### A-BASE (TI MODIFIED)

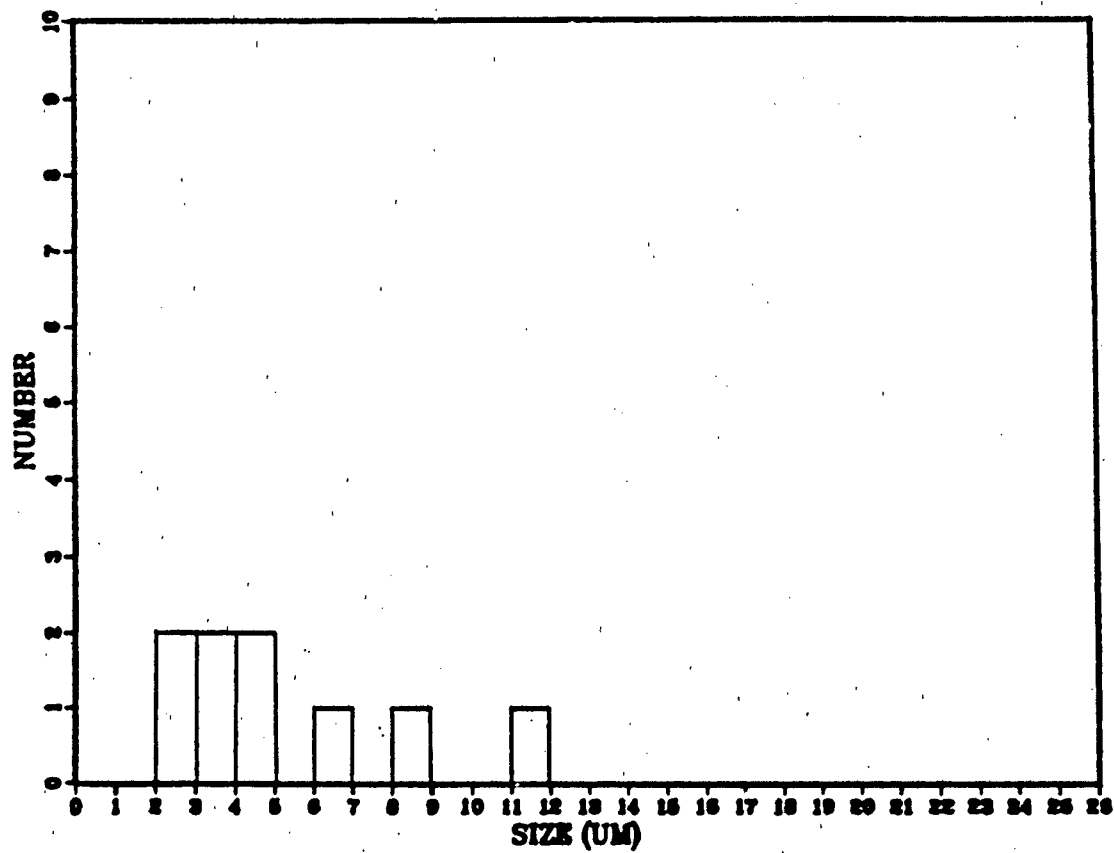


Figure 29. Oxide Inclusion distribution Ti Treated Parent Metal

### A-BASE (TI MODIFIED)

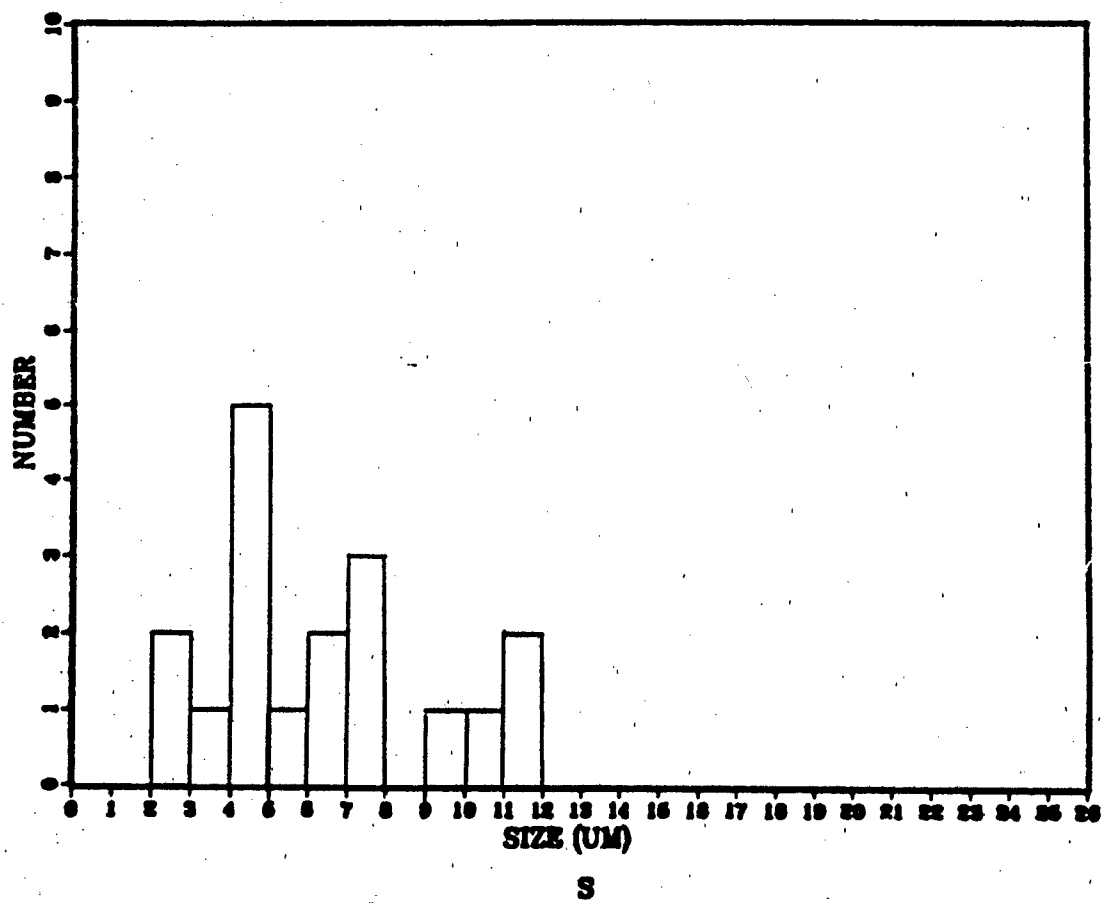


Figure 30. Sulfide Inclusion distribution TI Treated Parent Metal

### A-BASE WITH TI

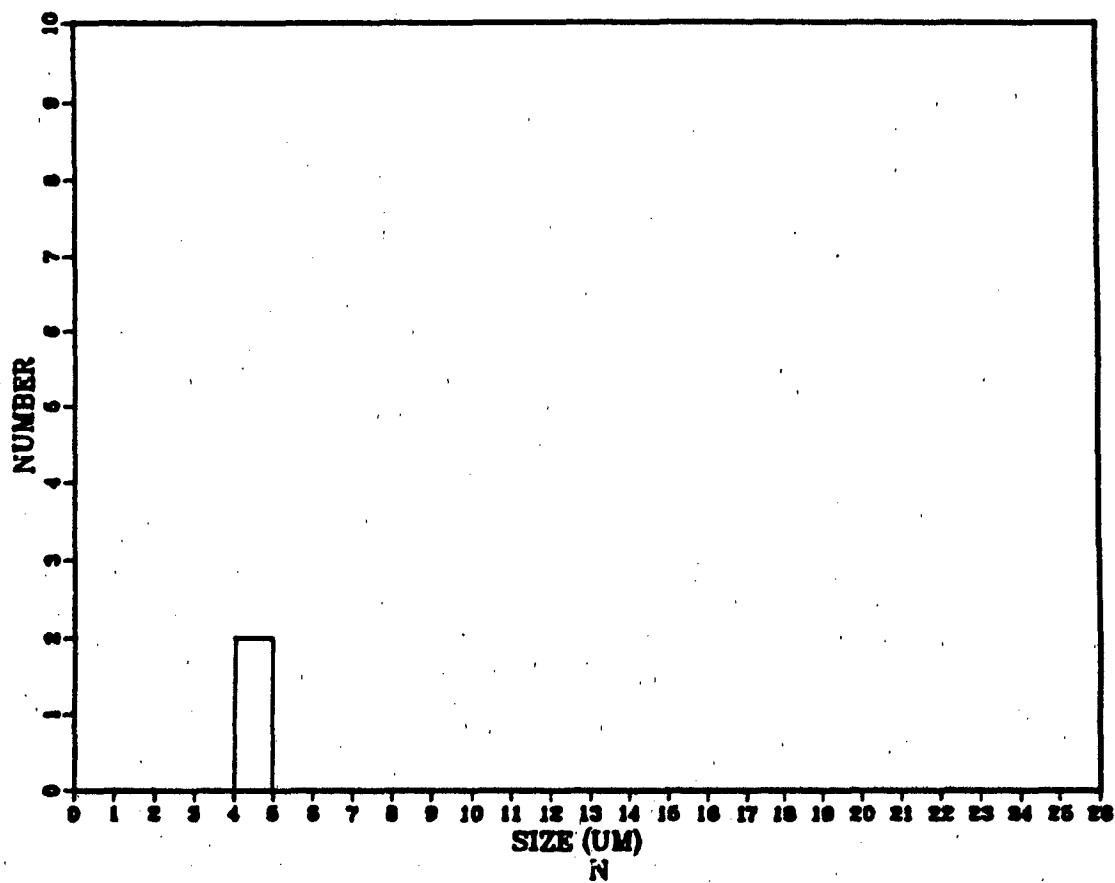


Figure 31. Nitride Inclusion distribution Ti Treated Parent Metal

### A-BASE WITH TI

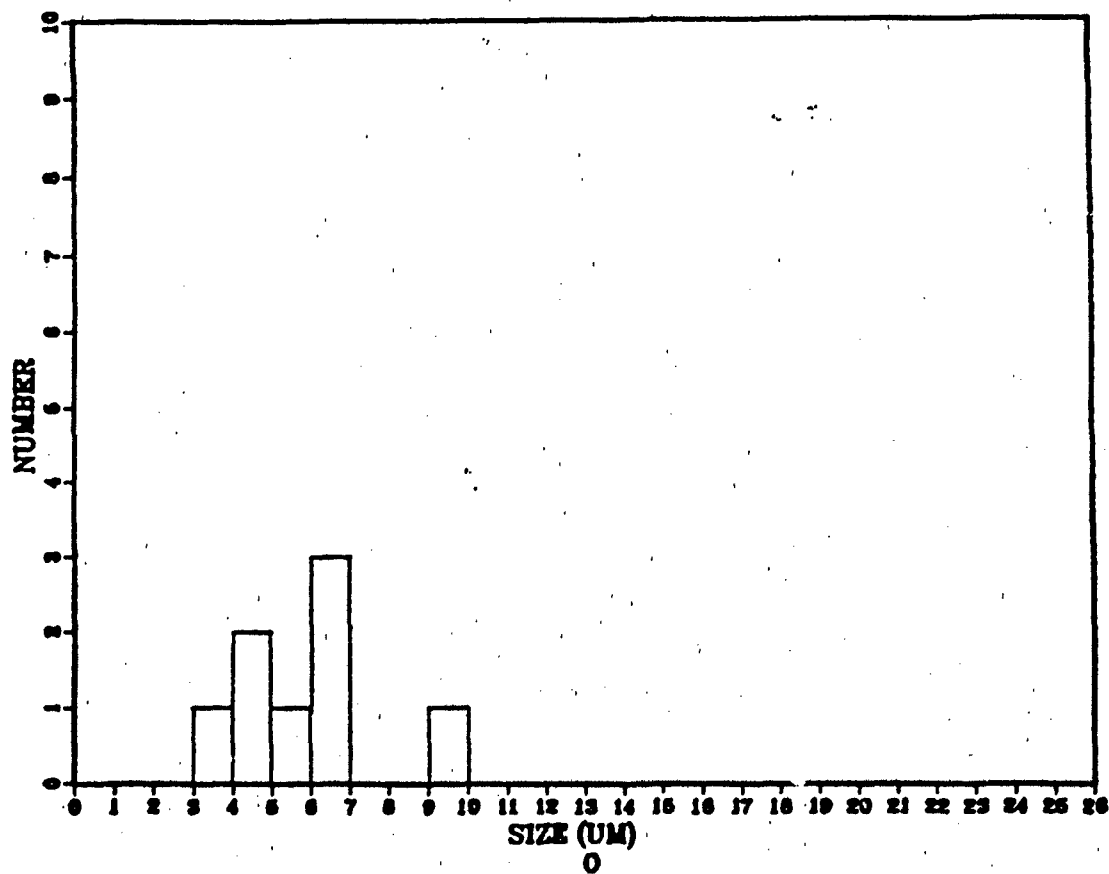


Figure 32. Oxide inclusion distribution Ti Treated HAZ, Weld, Parent

### A-BASE WITH TI

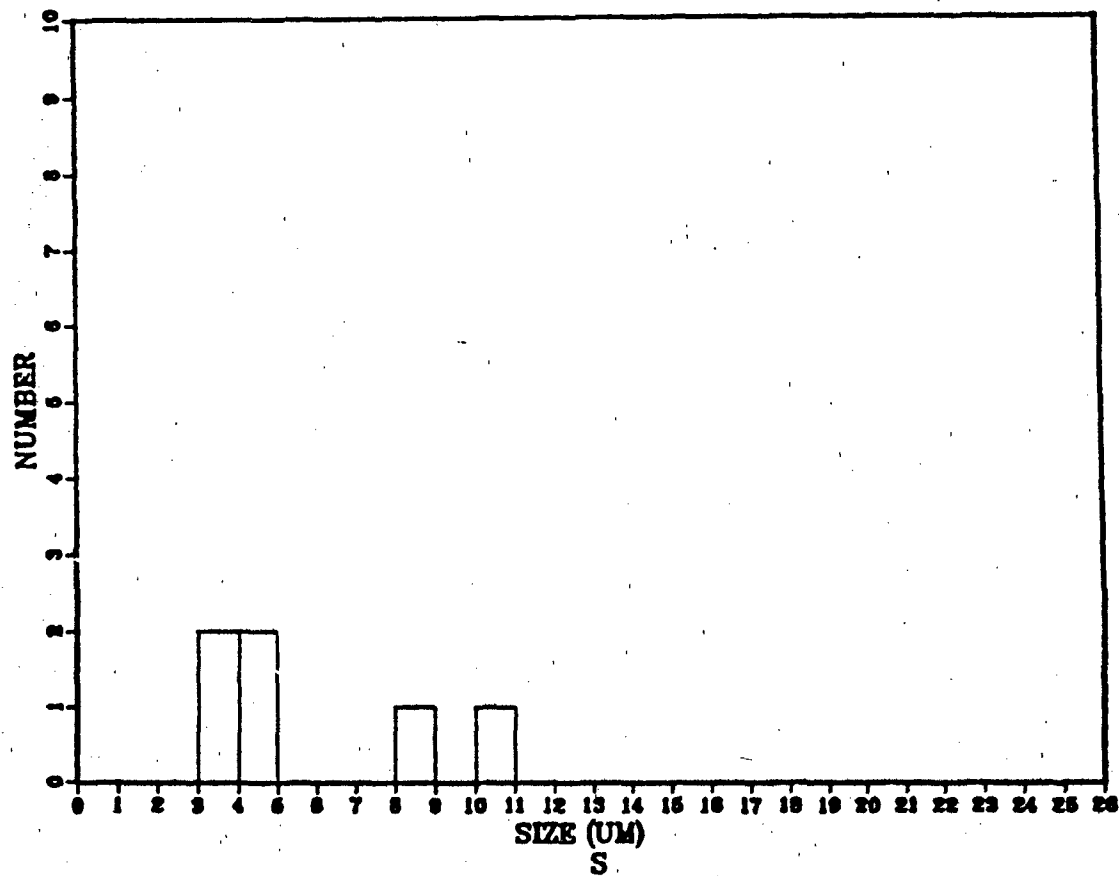


Figure 33. Sulfide inclusion distribution Ti Treated HAZ, Weld, Parent



### A-BASE WITH TI

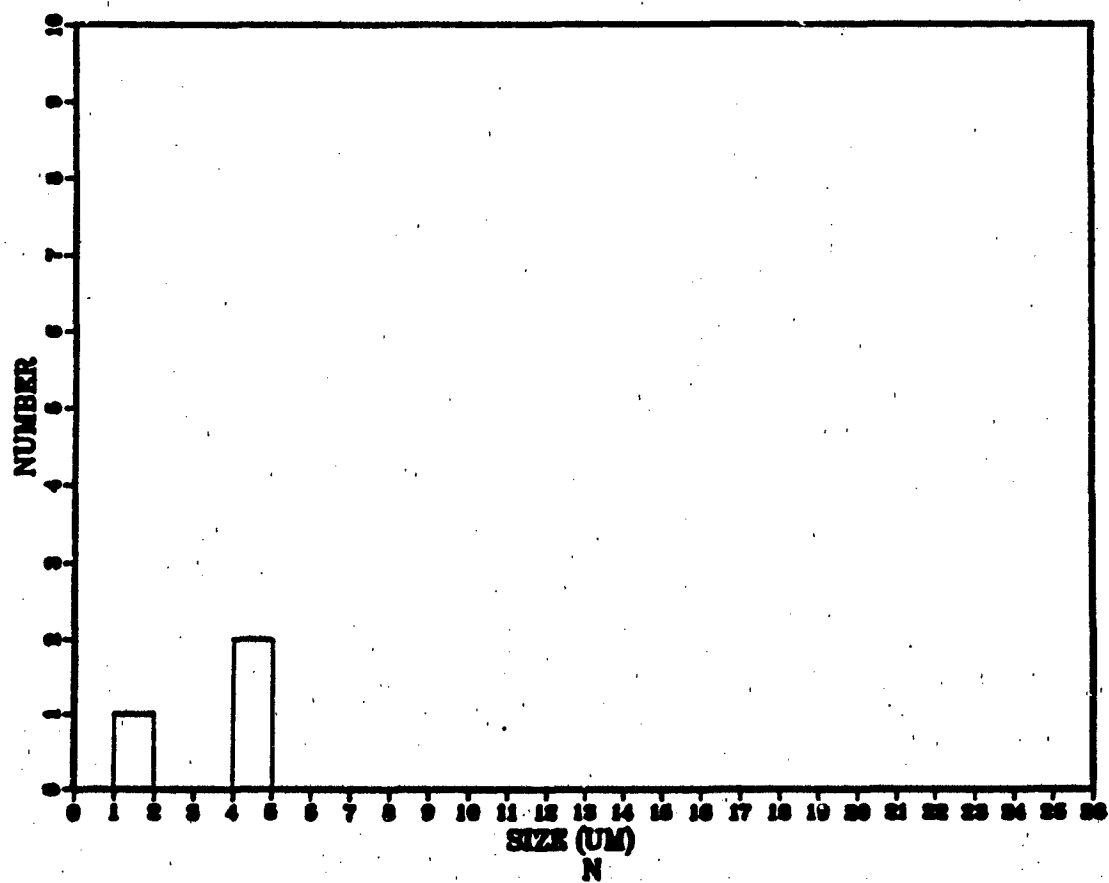


Figure 34. Nitride inclusion distribution Ti Treated HAZ, Weld, Parent

#### D. TRANSMISSION ELECTRON MICROSCOPY

The microstructure, characterized by TEM, is that of tempered martensite, tempered bainite in the HAZ. The parent metal revealed martensite and bainite microstructure. The TEM evaluation of the microstructure was done using the Ti-treated thin foil specimens, only because of lack of time.

##### 1. TEM Microscopy

###### *a. Ti Treated Parent Metal*

The fine dispersed interlath carbides are illustrated in Figure 35, and Figure 36 on page 57 shows the martensitic microstructure and Figure 37 on page 57 provides information regarding the bainite lath width.

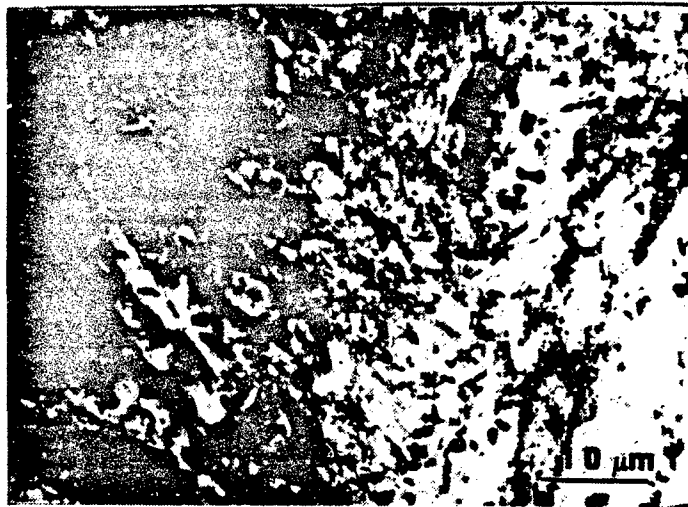


Figure 35. TEM Micrograph Ti Treated Parent Metal Interlath Carbides Dark Field Image

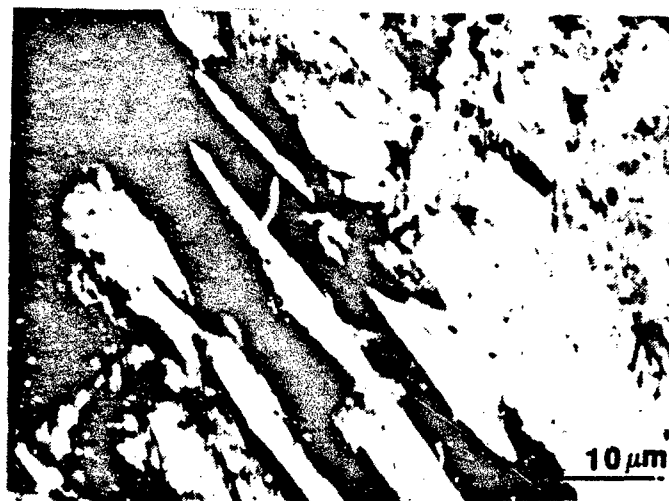


Figure 36. TEM Micrograph Ti Treated Parent Metal Martensite Bright Field Image

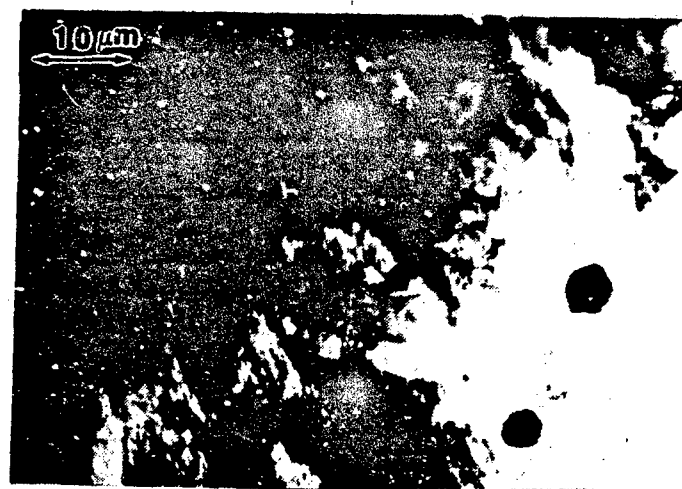


Figure 37. TEM Micrograph Ti Treated Parent Metal Bainite Lath's and Inclusions Dark Field Image

*b. Ti Treated HAZ*

Interlath carbides are illustrated in Figure 38 on page 58. In Figure 39 on page 58 the average bainite lath's width was measured, and a very inter-

esting micrograph of TiN inclusions that had been removed during electropolishing is shown in Figure 40 on page 59.

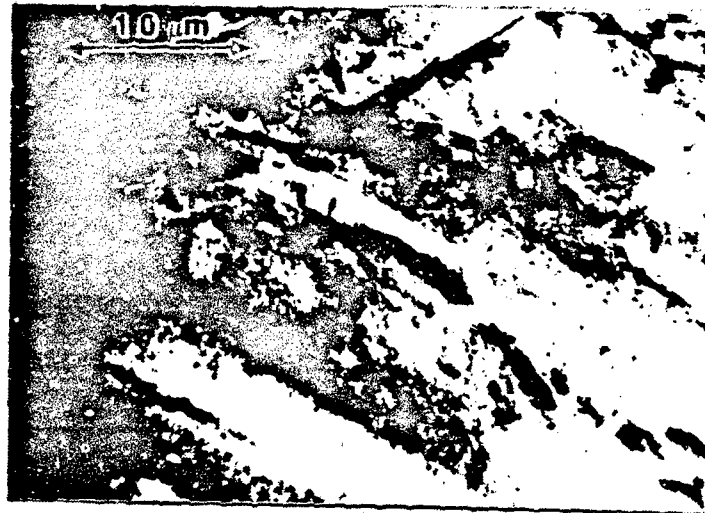


Figure 38. TEM Micrograph Ti Treated HAZ Interlath Carbides Bright Field Image



Figure 39. TEM Micrograph Ti Treated HAZ Bainite Lath's and Tempered Carbides Bright Field Image



Figure 40. TEM Micrograph Ti Treated HAZ Bainite Lath's and square TiN inclusion Bright Field Image

The average bainite lath width for the Ti apparent metal is about  $0.2\mu\text{m}$  refer to figure 37 and for the Ti HAZ it is approximately  $0.4\mu\text{m}$  refer to figure 39. The lath size will increase as the prior austenite grain size increases. In a packet of lath bainite all the laths have the same crystal orientation, and a crack can easily propagate through a cleavage plane. Thus, decreasing the bainite lath size will increase the number of crack interfaces and will increase the toughness of the material. The Ti treated samples revealed a much smaller prior austenite grain size. The primary means to reduce the prior austenite grain size, and increase toughness, is by the introduction of small non-metallic inclusions so that the grain boundaries are pinned. Through the use of fillers non-metallic inclusions can be readily introduced to the weld metal. Lau [Ref. 24] stated that the balance between titanium, aluminum, boron, oxygen, and nitrogen plays an important role in the inclusion population which influences the austenite to ferrite transformation by providing nucleation sites for ferrite or by pinning prior austenite grain boundaries.

Large inclusions are not effective in pinning austenite grain boundaries and prevent grain growth. However, TiN inclusions were so finely dispersed, they could not be detected within the grain boundaries. This could be due to the multipass GMAW process requires less heat than SA process and the TiN inclusions are redissolving. The higher the heat input it is found to promote growth of the particles because of the ex-

tended weld pool retention time (Grong et al., 1986, p.33). There was no evidence of grain boundary pinning by TiN or by a combination of Ti multiphase inclusions. This is primarily due to the thin area is not big enough to see significant number of prior austenite grain boundaries. Table 3 is a summary of SEM micrographs, TEM micrographs and EDX analysis for both the Ti and non Ti treated samples.

Table 3. SUMMARY OF RESULTS

Characteristics	Parent Metal		HAZ		HAZ, Parent Metal, Weld	
	Ti Treated	Non Ti Treated	Ti Treated	Non Ti Treated	Ti Treated	Non Ti Treated
Prior Austenite Grain Size	20 $\mu$ m	20 $\mu$ m	5 $\mu$ m	8 $\mu$ m	----	----
Lath Width	0.2 $\mu$ m	----	0.4 $\mu$ m	----	----	----
Lath Length (Packet)	10 $\mu$ m	18 $\mu$ m	4 $\mu$ m	5 $\mu$ m	----	----
Bainite Width Size (Packet)	3 $\mu$ m	4.8 $\mu$ m	4 $\mu$ m	6.7 $\mu$ m	----	----
Oxide inclusion maximum lot size	11 $\mu$ m	23 $\mu$ m	----	----	2 $\mu$ m	24 $\mu$ m
Nitride inclusion maximum lot size	6 $\mu$ m	----	----	----	4 $\mu$ m	----
Sulfide inclusion maximum lot size	11 $\mu$ m	20 $\mu$ m	----	----	10 $\mu$ m	24 $\mu$ m

---

### **E. MECHANICAL PROPERTIES**

The data provided from DTRC Charpy V-notch impact energy was plotted for Ti and non Ti samples refer to Figure 41 on page 62 and Figure 42 on page 63. From these results there needs to be more data points to give an accurate indication of the toughness in the HAZ and weld metal. However, from this data the toughness with the Ti treated material is higher than non Ti-treated.

# Ti MODIFIED HY-80 GMA

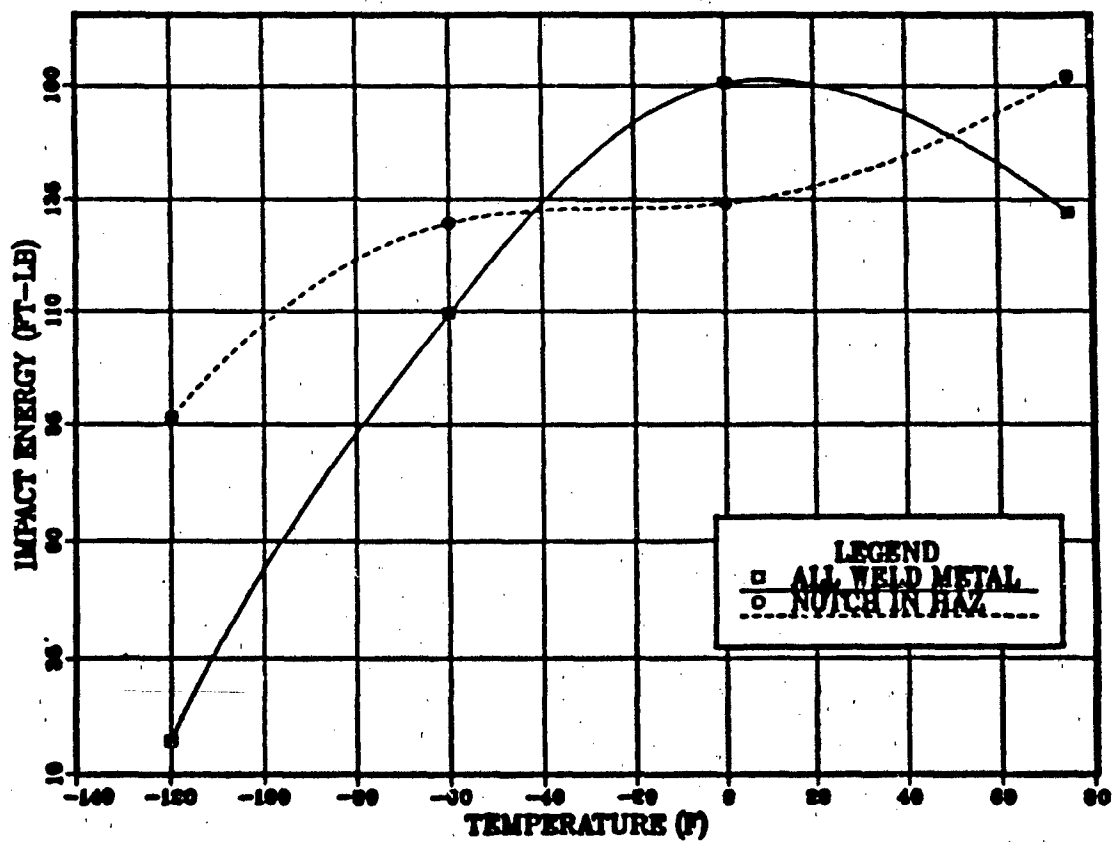


Figure 41. Charpy V-notch impact energy Ti-treated



# HY-80 GMA

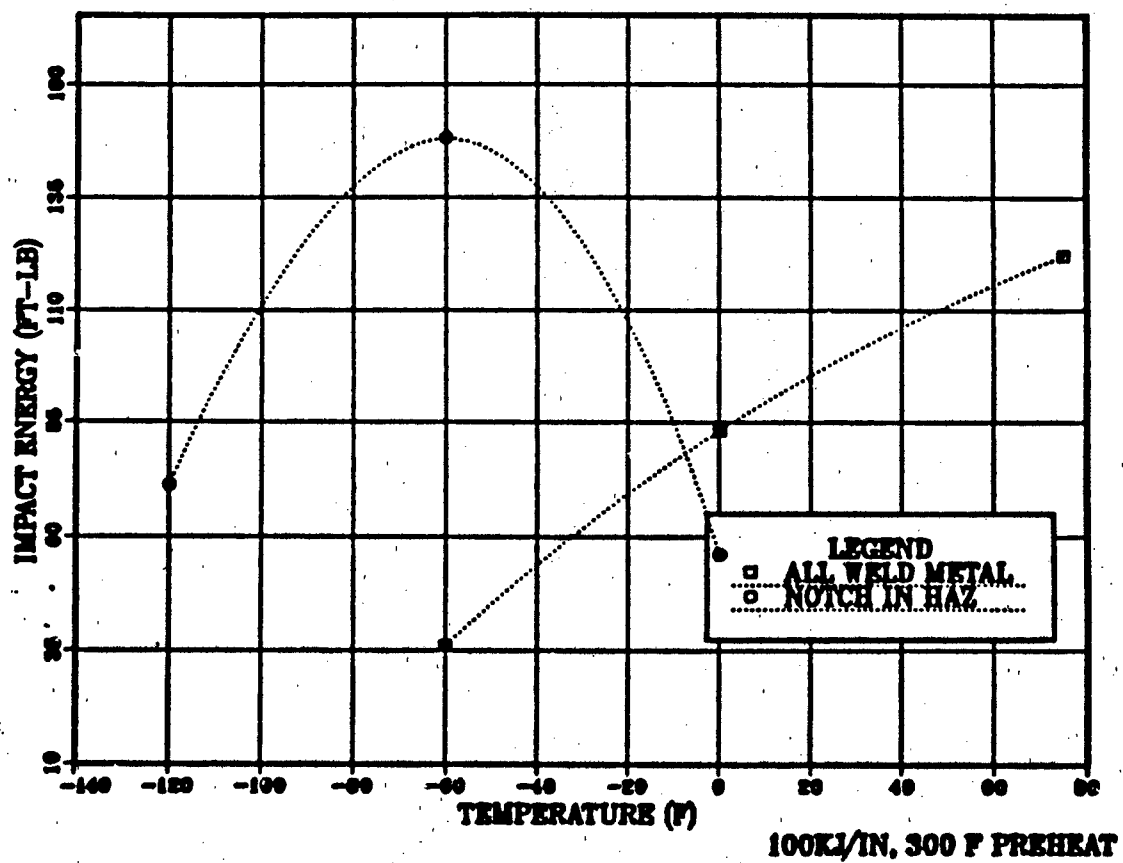


Figure 42. Charpy V-notch impact energy non Ti-treated

## **V. SUMMARY**

### **A. CONCLUSIONS**

Based on this investigation and results, the following conclusions can be drawn:

The inclusion size distribution will determine the final weld microstructure since non-metallic inclusions, pin prior austenite grain boundaries and refine lath structure.

The results of the SEM, EDX revealed that Ti reduces the uncombined oxygen level and assists calcium in sulfide shape modification.

That Ti treated samples produced a smaller prior austenite grain boundary and lath spacing than non Ti treated samples, thus increasing the toughness of the material.

That potential grain boundary pinning TiN inclusions were very fine, smaller than  $0.5\mu\text{m}$  and it was not possible to correlate these inclusions with prior austenite grain boundaries in the present work.

### **B. RECOMMENDATIONS**

The distribution and structure of inclusions in deposited weld metal is dependent on the flux used that will determine the level of toughness achieved through microstructural refinement. With further understanding the role of Ti inclusions in HAZ and its role in the nucleation of the final microstructure is still required. Utilizing carbon extraction replicas together with TEM observations to determine the size distribution, volume fraction, composition of inclusions and the correlation of TiN inclusions with prior austenite grain boundary pinning may prove beneficial in understanding how Ti forms nucleation sites and its effects on the microstructure.

## LIST OF REFERENCES

1. Farrar, R., Harrison, P., "Microstructural Development and Toughness of C-Mn and C-Mn-Ni Weld Metals Part II -Toughness," *Metal Construction*, pp. 39-42, August 1987.
2. Flax, F. W., Keith, R. G. and Randall, M. D., "Welding the Hy Steels," *ASTM Special Technical Publication 494, American Society for Testing and Materials*, Philadelphia, PA 1971.
3. Bell, A. R., "Properties of HY-130 Weldment Produced by Weld Pool Filler Synthesis," *Master's Thesis, Ohio State University*, 1985.
4. Burns, J. L., Moore, T. L. and Archer, R. S., "Quantitative Hardenability," *Transactions of the ASM*, v. 26, pp.1-22, March 1938.
5. Manganello, S. J., Dabkowski, D. S. and Gross, J. H., "Development of a High Toughness Alloy Plate Steel with a Minimum Yield Strength of 140ksi," *Welding Journal Research Supplement*, pp. 514s-520s, November 1964.
6. Shackleton, D. N., "The Welding of HY100 and HY130-Literature Review," *The Welding Institute*, pp. C287, 1972.
7. Dorsch, K. E., Lesnewich, A., "Development of a Filler Metal for a High-Toughness Alloy Plate Steel with a Minimum Yield Strength of 140 KSI," *Welding Journal Research Supplement*, pp. 564s-576s, December 1964.
8. Stout, R. D., Quattrone R., "Effects of Impurities on Properties of High Strength Steel Weld Metal," *Transactions of the ASM*, v. 47, pp. 785-793, November 1970.
9. Grong, O., Matlock, D. K., "Microstructural Development in Mild and Low-alloy Steel Weld Metals," *International Metals Review*, v. 31(1), 1986.

10. Matlock, D. K., Saverds, G. R., "The Metallurgy of HSLA Weld Metal Produced by the Submerged Arc Process," *Semiannual Technical Report, Department of Navy, Office of Naval Research*, Contract No N00014-83-K-0779, March 1985.
11. Edmonds, D. V., Cochrane, R. C., "Structure-Property Relationships in Bainitic Steels," *Metallurgical Transactions*, v. 21A, pp. 1527-1538, June 1990.
12. Kiessling, R., Lang, N., "Nonmetallic Inclusions In Steel," *The Metals Society, London*, 1978.
13. Pargeter, R. J., "Investigation of Submerged Arc Weld Metal Inclusions," *WIRR*, p. 151, 1981.
14. Tweed, J. H., Knotte, J. F., "Micromechanisms of Failure in C-Mn Weld Metal," *Acta Metallurgica*, v. 35(1), pp. 1401-1414, July 1987.
15. Gross, J. H., "The New Development of Steel Weldments," *Welding Journal Research Supplement*, pp. 241s-270s, June 1968.
16. Farrar, R., Harrison, P., "Influence of Oxygen-Rich Inclusions on the Gamma-Alpha Phase Transformation In High Strength Low Alloy Steel Weld Metals," *Journal of Material Science*, v. 16, 1981.
17. Reeves, M. C., "The Metallurgy of Welding of Carbon Low Alloy Steels," *The Joining of Metals*, p. 63, 1952.
18. *Welding Metallurgy*, John Wiley and Sons, p.230, 1987.
19. "Metals Handbook," 9th ed., v. 1, *American Society for Metals*, 1983.
20. Chen, C., Thompson, A. W. and Bernstein, I. M., "The Correlation of Microstructure and Stress Corrosion Fraction of HY-130 Steel Weldments," *Metallurgical Transactions*, v. 2A, p. 1613, September 1986.

- 
21. Elger, W. M., "Characterization of an HY-130 Steel Weldment of Transmission Electron Microscopy," *Master's Thesis, Naval Postgraduate School*, December 1981.
  22. Lancaster, J.F., "Metallurgy of Welding," 4th ed. *Allen and Unwin, London*, p.168, 1978.
  23. Dowling, J. M., Corbett, J. M. and Kerr, H. W., "Inclusions Phases and the Nucleation Acicular Ferrite in Submerged Arc Welds in High Strength Low Alloy Steels," *Welding Research Council*, v. 17A, p.1613, October 1980
  24. Lau, T. M., Burkart, J. and North, T. H., "Effect of Aluminum on the Ti-O-B-N Balance in Submerged Arc Welding," *Welding Journal*, pp.25-30, August 1988.

## INITIAL DISTRIBUTION LIST

	No. Copies
1. Defense Technical Information Center Cameron Station Alexandria, VA 22304-6145	2
2. Library, Code 52 Naval Postgraduate School Monterey, CA 93943-5002	2
3. Dr. Alan G. Fox, Code ME/Fo Department of Mechanical Engineering Naval Postgraduate School Monterey, CA 93943-5000	1
4. Mr. Ernest Czyryca, Code 2814 David Taylor Naval Ship Research and Development Center Annapolis, Md 21402-5067	1
5. Dana Jay Ellis 4937 Elks Dr. Columbus, OH 43214	2
6. Department Chairman, Code ME Department of Mechanical Engineering Naval Postgraduate School Monterey, CA 93943-5000	1
7. Department Engineering Curricular Office, Code 34 Department of Mechanical Engineering Naval Postgraduate School Monterey, CA 93943-5000	1

**END  
FILMED**

DATE: **12-91**

**DTIC**